Computer Methods and Programs in Biomedicine 270 (2025) 108950

Contents lists available at ScienceDirect

Computer Methods and Programs in Biomedicine

journal homepage: https://www.sciencedirect.com/journal/computer-methods-and-programs-in-biomedicine

LivXAI-Net: An explainable AI framework for liver disease diagnosis with IoT-based real-time monitoring support

Deepak Kumar [a,1], Brijesh Bakariya [a], Chaman Verma [b,*,1], Zoltan Illes [b,1]

[a] Department of Computer Application, IKGPTU, Jalandhar, 144603, Punjab, India
[b] Department of Media and Educational Informatics, Faculty of Informatics, Eötvös Loránd University, 1053 Budapest, Hungary

ARTICLE INFO

Keywords:
IoT
XAI
Liver disease prediction
Smart healthcare
Real-time monitoring
ML

ABSTRACT

Background & Objective : Liver disease remains a significant global health burden, often progressing silently until advanced stages such as cirrhosis or hepatic failure. Early detection is essential but remains hindered by the limitations of conventional diagnostics. This study presents LivXAI-Net, an explainable artificial intelligence (XAI) framework integrated with Internet of Things (IoT) biosensors, designed and evaluated in a simulated real-time setting using a historical dataset.

Methods: LivXAI-Net simulates continuous data acquisition from wearable biosensors — including sweat, platelet, and prothrombin sensors — and processes this data using machine learning (ML) models trained on the Mayo Clinic primary biliary cirrhosis (PBC) dataset (n = 424, 1974–1984). Random Forest (RF) and XGBoost(XGB) classifiers were deployed with SHAP and Permutation Feature Importance (PFI) to enhance interpretability. A mobile application, Hepatic Health Tracker, delivers real-time risk predictions, supported by a secure data pipeline using TLS 1.3 and AES-256 encryption.

Results: RF and XGB achieved accuracies of 84% and 82% respectively under 20-fold cross-validation. Key biomarkers — albumin, cholesterol, and triglycerides — were consistently identified by SHAP as influential in classification. The system achieved a total latency of 0.85 s in a simulated 5G environment, supporting near-instantaneous alert delivery via the mobile interface.

Conclusion: LivXAI-Net combines interpretable ML with real-time biosensor data to enable proactive liver disease management. While currently validated using historical data in a simulated environment, future work will involve deployment with live sensor input and clinical trials to validate utility and generalizability in real-world settings.

1. Introduction

Liver disease is a major global health challenge, contributing significantly to morbidity and mortality worldwide. The liver plays a critical role in metabolism, detoxification, and immune regulation, making early detection of liver dysfunction essential for preventing severe complications. However, traditional diagnostic methods — such as liver function tests, imaging scans, and biopsies — often fail to identify liver disease in its early stages, delaying intervention and limiting treatment effectiveness [1]. This paper primarily focuses on the development and validation of LivXAI-Net, an XAI framework for liver disease diagnosis. The IoT and 5G architecture are discussed as supportive components to enable real-time deployment, but the main contribution lies in the XAI-based diagnostic model and its clinical interpretability [2]. While the proposed system is currently tested using historical data, real-time implementation with IoT sensors and 5G connectivity is planned for future clinical validation.

The IoT has transformed healthcare by enabling continuous, real-time patient monitoring through Body Sensor Networks (BSNs) [3]. These networks, consisting of wearable and implantable biosensors, allow for the constant tracking of vital health parameters such as body temperature, blood pressure, respiration rate, and liver enzyme levels. When combined with cloud computing, IoT-powered healthcare systems facilitate remote monitoring, enabling timely medical interventions and improving patient outcomes [4]. Additionally, IoT-driven healthcare enhances operational efficiency by optimizing data management, improving early disease detection, and supporting proactive patient monitoring [5].

* Corresponding author.
E-mail addresses: Dr.D.K.Mehta81@gmail.com (D. Kumar), Dr.Brijeshbakariya@ptu.ac.in (B. Bakariya), chaman@inf.elte.hu (C. Verma), illes@inf.elte.hu (Z. Illes).

[1] Deepak Kumar's work belongs to his Ph.D. study. Chaman Verma and Zoltan Illes work belongs to the faculty of informatics at Eotvos Lorand University, Hungary.

https://doi.org/10.1016/j.cmpb.2025.108950
Received 17 February 2025; Received in revised form 24 June 2025; Accepted 6 July 2025
Available online 18 July 2025

IoT-based remote health monitoring has proven effective in managing chronic diseases, particularly in cardiovascular and metabolic disorders. For instance, continuous glucose monitors (CGMs) track real-time fluctuations in blood sugar levels, significantly improving diabetes management [6]. Similarly, smart heart monitors (e.g., Apple Watch ECG, Holter monitors) have enhanced the early detection of cardiac arrhythmias, enabling rapid intervention and reducing hospitalizations [7]. However, despite these advancements, IoT applications for liver disease remain underdeveloped. Unlike cardiovascular diseases, where wearable monitoring solutions are widely adopted, liver disease often progresses silently until it reaches an advanced stage, making early detection more challenging [8]. Real-time liver biomarker monitoring through IoT could bridge this gap, allowing for timely intervention before irreversible liver damage occurs. IoT-driven, real-time liver biomarker monitoring could bridge this gap, allowing for early detection and preventative healthcare interventions before irreversible liver damage occurs [9].

Recent studies have validated the effectiveness of ML models [10] in liver disease diagnosis. For example, A.J.M. Rani et al. [11] employed a hybrid Support Vector Machine classifier (SVC) with K-Means clustering for liver disease severity classification, successfully identifying affected patients. Similarly, K.Prakash et al. [12] utilized deep learning models, including Convolutional Neural Networks (CNNs) and ensemble learning, achieving 98.8% accuracy. Additionally, S.A. Farooq et al. [13] applied a RF classifier for multi-class liver disease classification, attaining 93.5% accuracy.

While these ML models demonstrate high predictive performance, they suffer from a lack of interpretability, limiting their integration into clinical decision-making [14]. In medical applications, a significant challenge in AI adoption is the black-box nature of many ML models, which provide accurate predictions without explaining their reasoning. This lack of transparency reduces trust among healthcare professionals, who require clinically interpretable models to validate AI-driven diagnoses [15].

To address this, XAI techniques such as SHAP and PFI offer clear justifications for AI-driven predictions [16]. For instance, SHAP analysis can highlight key biomarkers influencing liver disease classification, such as bilirubin, albumin, and cholesterol levels. By providing clinicians with interpretable explanations, XAI enhances trust, adoption, and decision-making reliability in AI-assisted liver disease diagnosis [17].

Liver diseases are broadly classified into hepatocellular, cholestatic, and infiltrative types, based on enzyme activity [18]. Copper distribution studies have been instrumental in differentiating liver conditions, particularly in cases such as Wilson's disease and primary biliary cirrhosis [19]. Among liver disorders, fatty liver disease is a key precursor to fibrosis and is strongly associated with metabolic risk factors such as obesity and diabetes [20,21]. Cirrhosis, a frequent consequence of chronic hepatitis B infection and biliary diseases, can lead to severe complications, including portal hypertension and liver failure, if left untreated [22]. Hepatic failure, often triggered by infections, toxins, or drug-induced liver injury, necessitates urgent medical intervention [23]. Liver disease progression typically follows a trajectory from steatosis and fibrosis to cirrhosis and hepatic failure, with chronic viral hepatitis contributing significantly to the global disease burden [24]. Advances in ML-driven liver disease diagnosis have shown promise in improving early detection and treatment outcomes.

Despite significant progress in AI-driven healthcare, most existing IoT-based liver disease monitoring systems emphasize data collection and automation over explainability, restricting their adoption in clinical settings [15]. To address this gap, this study introduces LivXAI-Net, an IoT-XAI-powered framework for real-time monitoring and predictive analysis of liver disease progression. The proposed system integrates:

- **IoT sensors** for continuous health parameter tracking,
- **Cloud-based AI models** for predictive analytics, and
- **Explainability techniques**, such as Permutation Feature Importance (PFI) and SHAP, to enhance AI interpretability [25,26].

The LivXAI-Net framework enables secure data transmission, AI-driven analysis, and real-time medical alerts while ensuring decision-making transparency. Additionally, it incorporates robust encryption protocols to maintain privacy and security.

Fig. 1 illustrates the end-to-end workflow of the proposed IoT-XAI-based healthcare system. IoT sensors collect real-time patient data, which is transmitted to a cloud-based system for processing. The data undergoes cleaning and feature extraction before being analyzed using XAI models. The model's predictions, along with interpretable explanations (e.g., SHAP and PFI), are then shared with patients, doctors, and hospitals via mobile alerts and dashboards. This ensures transparency, security, and timely medical intervention.

By combining PFI and SHAP, the framework generates clinically relevant explanations [16], fostering greater trust and transparency in AI-assisted medical decision-making. Additionally, to ensure patient data privacy, the system integrates secure encryption and access control mechanisms.

A crucial aspect of developing a robust liver disease stage prediction model is the quality of clinical data used for training and validation. Many existing liver disease datasets primarily focus on demographic and lifestyle factors, limiting their clinical depth. In contrast, this study leverages a longitudinal dataset from the Mayo Clinic (1974–1984), which contains detailed clinical records of PBC patients. This dataset includes 424 patient records with 19 clinical attributes and an extended follow-up period ranging from 41 to 4795 days (average: 1917 days), making it particularly valuable for survival analysis and predictive modeling [27–29]. By incorporating comprehensive biomarker and disease progression data, this dataset enhances the reliability of the proposed AI-driven diagnostic framework.

1.1. Contribution

This study introduces LivXAI-Net, an IoT-XAI-powered framework designed to enhance real-time liver disease monitoring and predictive analytics. The unpredictable progression of liver disease necessitates continuous tracking and AI-driven decision support to enable early intervention and improved patient outcomes. The key contributions of this research include:

- A hybrid explainability pipeline combining SHAP and PFI is introduced for both global and instance-level interpretation of liver disease predictions.
- A simulated IoT healthcare workflow is designed using wearable biosensors (e.g., sweat, platelet, prothrombin sensors) for continuous monitoring on NS3 Simulator, achieving low-latency (0.85s on 5G) data transmission and real-time alerts.
- Deploys explainability-driven AI within a simulated IoT healthcare workflow to evaluate real-time response feasibility using historical liver disease data.
- Integrates clinical domain knowledge into model interpretation, enabling feature-attribution insights that align with liver pathology (e.g., Albumin and Prothrombin tracking).
- Embeds SHAP explanations directly into a mobile interface for clinician-patient interaction, advancing AI transparency in real-world healthcare tools.

In summary, the proposed framework accurately classifies liver disease stages (Steatosis, Cirrhosis, and Hepatic Failure) while ensuring interpretability and real-time decision support. Upon detecting abnormalities, the system generates clear, interpretable explanations and transmits alerts to both patients and healthcare providers, enabling early intervention and improved clinical outcomes.

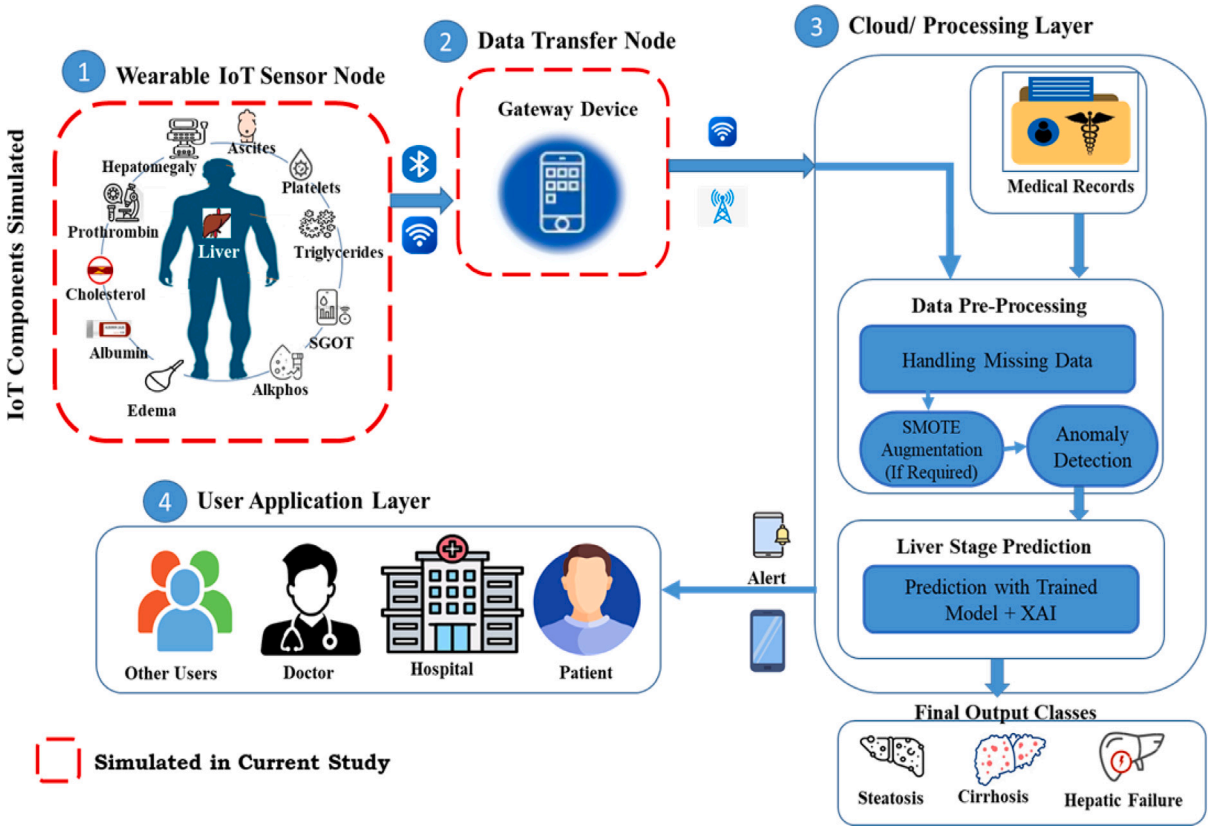

Fig. 1. Workflow overview.

1.2. Paper organization

The remainder of this paper is structured as follows:

- Section 2: Related Work Reviews existing IoT-based frameworks for liver disease prediction, highlighting their strengths, limitations, and the need for explainable AI in clinical decision-making.
- Section 3: Proposed LivXAI-Net Framework Details the architecture of the proposed system, including IoT sensor integration, cloud-based AI processing, and explainability techniques (SHAP & PFI) to enhance model transparency.
- Section 4: Experimental Setup and Methodology Describes the dataset used for model training and validation, data preprocessing techniques, anomaly detection methods, ML model selection, and hyperparameter tuning strategies.
- Section 5: Results and Discussion Presents the performance evaluation of different ML models (RF, XGB, SVC, and Logistic Regression(LR)) using accuracy, precision, recall, and AUC scores, followed by a comparison with deep learning models to contextualize accuracy versus explainability trade-offs. Also includes an explainability analysis using SHAP to identify key biomarkers influencing liver disease classification.
- Section 6: Mobile Application Development Introduces the Hepatic Health Tracker, a mobile application for real-time patient monitoring and alert notifications, describing its user interface, backend architecture, and real-time data processing capabilities.
- Section 7: Conclusion and Future Directions Summarizes key findings, clinical implications, and areas for future research, including blockchain integration for enhanced data security, edge computing for scalability, and real-world validation through hospital trials.

2. Related work

The application of Artificial Intelligence (AI) and IoT in healthcare has expanded significantly, covering areas such as disease prediction [30], outbreak forecasting, personalized medicine [31], fraud detection, and remote patient monitoring [32]. In particular, AI-powered IoT frameworks have demonstrated great potential in liver disease prediction and management, where ML and deep learning (DL) models enhance diagnostic accuracy and enable early intervention. This section reviews key studies integrating IoT with ML/DL for liver disease prediction, alongside related advancements in XAI.

Yoon Kim et al. [33] examined the role of an mHealth application and wearable device in providing personalized rehabilitation exercises for hepatocellular carcinoma (HCC) patients, demonstrating its effectiveness in post-therapy recovery. While mHealth applications like those proposed by Yoon Kim et al. demonstrate the potential of personal devices in healthcare, the adoption of BYOD policies remains limited in clinical practice due to concerns over data security and device compatibility. LivXAI-Net addresses these barriers by integrating robust security protocols and a modular architecture, positioning BYOD as a viable component for future IoT-driven healthcare systems. Similarly, Andreas Voss et al. [34] developed a wearable electronic nose system utilizing semiconductor metal oxide sensors to detect liver dysfunction by analyzing exhaled breath, effectively distinguishing compensated from decompensated cirrhosis. Kaidong Wang et al. [35] introduced a non-invasive technique for early-stage non-alcoholic fatty liver disease (NAFLD) detection using an on-skin impedance sensor combined with an attention-based deep learning algorithm, achieving an accuracy of 97.5% with an AUC of 1.0.

Recent studies have applied XAI and IoT techniques to enhance healthcare diagnostics across various conditions, offering insights relevant to liver disease monitoring. For instance, Khan et al. [40] developed D2PAM, a deep learning model using attention mechanisms

Table 1
Comparative analysis of selected studies, assessing key features including dataset properties, AI methodologies, real-time monitoring, XAI integration, and patient alert mechanisms.

Paper	A	B	C	D	E	F	G	H	Limitations
Sengupta et al. (2022) [36]	Acute Liver Failure (8785 instances)	RF,XGB, LGBM	✓	×	×	×	×	×	Only prediction algorithm with random oversampling technique
Khan et al. (2020) [37]	Hungarian Heart Disease (2941), Framingham (4240)	MDCNN	×	✓	✓	×	×	✓	Ambiguity in IoT layer understanding, missing patient alerts
Hannan et al. (2024) [38]	Tertiary heart disease (1000)	RF,XGB, SVC	×	×	✓	×	✓	✓	Limited evaluation metrics, lack of deployment details
Farooq et al. (2023) [13]	HCV (615)	RF, XGB	×	×	×	×	×	×	Missing oversampling technique in multiclass classification, no XAI integration
Kumar et al. (2021) [39]	HF (299)	RF, GBM, LR, XGB	×	✓	✓	×	✓	✓	XAI and app deployment are missing

Note: Columns C, D, E, F, G, H represent IoT Integration, XAI Usage, Real-Time Monitoring, Patient Alerts, Mobile App Integration, and Comprehensive Evaluation Metrics, respectively.

for epileptic seizure prediction from EEG data, emphasizing interpretability to address patient variability. Similarly, their Dual-3DM3-AD model [41] integrates MRI and PET scans with XAI for transparent Alzheimer's diagnosis. In breast cancer detection, Alhussen et al. [42] proposed XAI-RACapsNet, leveraging XAI and heat maps to improve mammogram analysis transparency. These works highlight the broader applicability of XAI and IoT in healthcare, providing interpretable, real-time diagnostic solutions that inform the design of LivXAI-Net for liver disease.

For liver disease prediction, LivMarX, an ML-driven model by K.K. Sudiksha et al. [43], achieved 86% accuracy and an AUC of 0.95 in predicting liver cirrhosis stages using biomarkers, providing a cost-effective alternative to imaging-based diagnostics. Additionally, Sai et al. [44] proposed an AI-driven digital twin framework integrating IoT and NFTs for chronic disease management, enabling remote monitoring and personalized care through ML-based drug recommendations, disease stage detection, and nutrition management.

Sengupta et al. [36] demonstrated the effectiveness of RF and LightGBM (LGBM) classifiers in predicting acute liver failure, achieving 99.3% cross-validation accuracy and a 99.6% F1-score, highlighting the potential of computational models in clinical decision-making. Similarly, Prakash & Saradha [12] applied deep learning models, including CNNs and ensemble learning, achieving 98.8% accuracy. However, a major limitation was the lack of interpretability, reducing clinical trust in the AI predictions.

Perumal et al. [45] developed Tri-M2MT, a multi-modal MRI-based model for diagnosing Acute Bilirubin Encephalopathy in neonates, using advanced capsule networks and transformer architectures to ensure interpretable feature extraction and fusion, which aligns with the need for transparent AI in healthcare. Similarly, Kujur et al. [46] explored CNN and PCA-CNN models for brain MRI classification, demonstrating that models like InceptionV3 achieve high accuracy while maintaining computational efficiency, offering lessons for optimizing IoT-based real-time diagnostics. These studies underscore the potential of XAI and efficient architectures to inform the interpretable, scalable design of LivXAI-Net for liver disease diagnosis.

Despite these advancements, many studies have overlooked key clinical markers such as the prothrombin ratio, which is an essential indicator of liver function. This ratio reflects the liver's ability to synthesize clotting factors and serves as a valuable non-invasive marker for liver fibrosis and cirrhosis severity. Croquet et al. [47] validated the prothrombin index as a fibrosis marker, while Mahmud et al. [48] incorporated it into a predictive model for postoperative mortality in cirrhotic patients, demonstrating its clinical relevance. However, studies such as Zhang et al. [49] failed to include prothrombin time, limiting their ability to accurately stratify disease progression.

Recent studies identify the HbA1c/HDL-C ratio as a strong biomarker for MAFLD risk, showing a significant positive correlation with disease prevalence. The association follows a nonlinear pattern, with a defined threshold beyond which the risk increases sharply, emphasizing its potential for early detection and screening [50]. Liver fibrosis, driven by hepatic stellate cell activation, cytokine release, and excessive collagen deposition, often progresses to cirrhosis, portal hypertension, or hepatocellular carcinoma [51]. Early detection of liver disease stages, combined with interpretable ML models, is crucial for improving patient prognosis. This study builds on prior research by integrating XAI techniques, such as SHAP and PFI, into an IoT-based healthcare framework to provide transparent and clinically interpretable predictions.

Liver biopsy remains the definitive method for evaluating hepatic injury and fibrosis in chronic hepatitis, leading to the widespread use of standardized histological scoring systems. Among these, the Histology Activity Index (HAI) proposed by Ishak and the METAVIR system (Meta-analysis of Histological Data in Viral Hepatitis) are the most frequently employed [52].

2.1. Research gap identification

Despite advancements in AI-driven liver disease prediction, several limitations persist, as outlined in Table 1. One major issue is the limited integration of external data sources, which restricts AI models from comprehensively analyzing high-dimensional clinical data [36]. Many existing studies rely on small, isolated datasets, reducing the generalizability and robustness of predictive models. Additionally, the lack of oversampling techniques in certain studies has led to class imbalance problems, where minority class instances are underrepresented, affecting prediction accuracy in multiclass liver disease classification [13]. Another critical limitation is the ambiguity in IoT layer implementation, particularly in studies where patient alert mechanisms are inadequately defined [37]. Without a clear IoT architecture, real-time monitoring becomes inefficient, and urgent medical alerts may not be effectively communicated to healthcare providers or patients. Moreover, while AI models demonstrate high predictive accuracy, the absence of XAI methodologies reduces transparency and clinician trust [39]. Without interpretable AI frameworks, healthcare professionals may struggle to validate predictions and understand the reasoning behind model outputs, limiting real-world adoption. Furthermore, many studies employ limited evaluation metrics, often focusing solely on accuracy while neglecting AUC, precision–recall, and sensitivity-specificity metrics, which are crucial for assessing model reliability and clinical applicability [38].

To further underscore the novelty of LivXAI-Net, we compare it with prior IoT-based liver disease studies, particularly those leveraging advanced sensing and AI techniques. For instance, Wang et al. [35] developed a non-invasive impedance sensor system for early-stage non-alcoholic fatty liver disease (NAFLD) detection, achieving a robust 97.5% accuracy with an AUC of 1.0 using an attention-based deep learning model. While highly accurate, their approach focuses solely on NAFLD detection, lacks real-time monitoring capabilities, and does not incorporate explainability, limiting its clinical interpretability.

Table 2
Novel contributions summary.

Study	XAI method	IoT integration	Mobile app	Dataset type	Novel contribution
Kim et al. (2021) [33]	None	Yes	Yes	Real World	Post-therapy rehabilitation
Wang et al. (2022) [35]	Attention-based DL	Yes	No	Impedance Sensors	NAFLD Detection
Sengupta et al. (2022) [36]	None	No	No	Structured	High accuracy, no XAI
Our Study (LivXAI-Net)	SHAP + PFI	Simulated with NS3	Yes	Longitudinal Clinical	Explainable, real-time monitoring

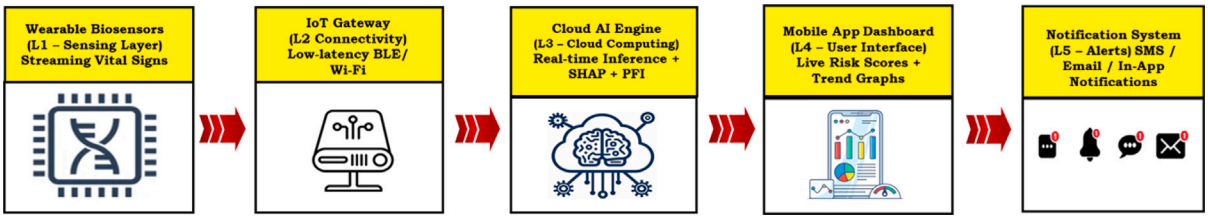

Fig. 2. High-Level System Architecture of LivXAI-Net showing its layered structure (sensing, connectivity, cloud computing, user interface, and alert system).

In contrast, LivXAI-Net integrates IoT-enabled wearable biosensors (e.g., sweat, platelet, and prothrombin sensors) for continuous, real-time monitoring of multiple liver disease stages — Steatosis, Cirrhosis, and Hepatic Failure — achieving a robust 84% accuracy on 20-fold (Table 5) with low latency (0.85s on 5G) for end-to-end processing in a simulated IoT environment, including data transmission and model inference. By employing SHAP and PFI (Figs. 5–8), LivXAI-Net provides both instance-level and global feature attribution, identifying key biomarkers (e.g., Albumin, Cholesterol, Triglycerides) that align with clinical standards like NAFLD Activity Score (NAS) and Child-Pugh, thus enhancing trust and adoption among clinicians.

Similarly, Voss et al. [34] utilized a wearable electronic nose system to detect liver dysfunction via exhaled breath, distinguishing compensated from decompensated cirrhosis. While innovative, their system is limited to binary classification and lacks IoT integration for continuous data streaming or XAI for transparent predictions. LivXAI-Net overcomes these limitations by offering multiclass classification across three liver disease stages, supported by a five-layer IoT architecture (Fig. 3) that ensures secure, real-time data transmission and processing. Additionally, unlike Kim et al. [33], which focused on post-therapy rehabilitation for hepatocellular carcinoma using mHealth without predictive analytics, LivXAI-Net provides proactive disease stage prediction and automated alerts via a mobile app (see Section 6), enabling early intervention.

The dual emphasis on predictive accuracy and explainability, coupled with real-time IoT integration, distinguishes LivXAI-Net from prior IoT-liver studies. While studies like Wang et al. [35] and Sengupta et al. [36] achieve higher accuracy (97.5% and 99.3%, respectively), their lack of real-time monitoring and interpretability restricts clinical utility. LivXAI-Net's hybrid XAI pipeline (SHAP and PFI) and mobile app integration (Figs. 11–12) bridge this gap, offering a clinically relevant, transparent, and scalable framework for liver disease management, as summarized in Table 2.

To address these challenges, our study integrates several key improvements. First, we implement real-time monitoring using IoT-connected sensors, enabling continuous patient tracking and early disease detection. Second, we incorporate external data sources to create a more comprehensive and diverse dataset, enhancing model robustness and generalizability. Third, we apply state-of-the-art XAI techniques, including SHAP and PFI, to improve AI transparency and interpretability, making predictions more clinically meaningful. Additionally, we employ comprehensive evaluation metrics, including AUC, F1-score, and precision–recall analysis, to ensure the reliability and clinical validity of our framework. Lastly, we integrate an automated patient alert system using SMS, email, and mobile notifications, ensuring timely medical intervention and improved patient care. By addressing these existing research gaps, this study presents an IoT-XAI-powered liver disease monitoring system that not only enhances predictive performance but also ensures explainability, real-time intervention, and better patient outcomes.

Unlike prior work that emphasizes predictive performance or IoT integration alone, our framework uniquely combines real-time responsiveness with interpretable, clinically grounded outputs via a mobile platform as discussed in Table 2. This enables both AI transparency and prospective deployment readiness.

3. Proposed LivXAI-Net framework

To address the need for explainable and secure liver disease monitoring, we propose LivXAI-Net, a multi-layered IoT-XAI framework integrating wearable biosensors, cloud-based analytics, and real-time alert systems. Fig. 2 presents an overview of the proposed framework, highlighting its architectural components and data flow. This high-level depiction provides essential context for understanding the more detailed layer-specific implementations described later in this section. Fig. 3 further elaborates on the conceptual workflow of the system, including cloud processing and mobile interface integration.

With growing patient awareness and the increasing demand for cost-effective, high-quality healthcare, seamless access to personal health records has become essential. Emerging technologies such as cloud computing, IoT, and Bring Your Own Device (BYOD) policies have the potential to facilitate secure data sharing and inter-service collaboration, driving transformative advancements in healthcare. While BYOD is not yet widely adopted in clinical practice due to security and interoperability challenges, LivXAI-Net incorporates it as a prospective feature to enhance patient accessibility, supported by robust security measures (e.g., TLS 1.3, AES-256 encryption, and RBAC) to address these concerns [53]. However, ensuring the explainability and transparency of AI-driven decisions in medical applications remains a challenge. To address this, we propose an explainable IoT-based framework for liver disease stage identification, integrating real-time monitoring and predictive analytics. The framework delivers timely insights via a mobile app, SMS, or email alerts, enhancing proactive disease management. It is structured into four key layers, as illustrated in Fig. 1, with a detailed explanation provided in Fig. 3.

The framework consists of development, testing, and production phases, where sensor and electronic medical record (EMR) data are used for model training, tuning, and validation. Withheld data assesses performance and generates explainability through XAI methods, guiding feature selection for refinement. A key feature of the framework is its integrated XAI component, enhancing transparency and ensuring optimal deployment in the cloud for real-world applications. The choice of SHAP and PFI in LivXAI-Net leverages their complementary strengths—SHAP for local, instance-specific explanations useful in clinical decisions, and PFI for global, model-agnostic feature importance.

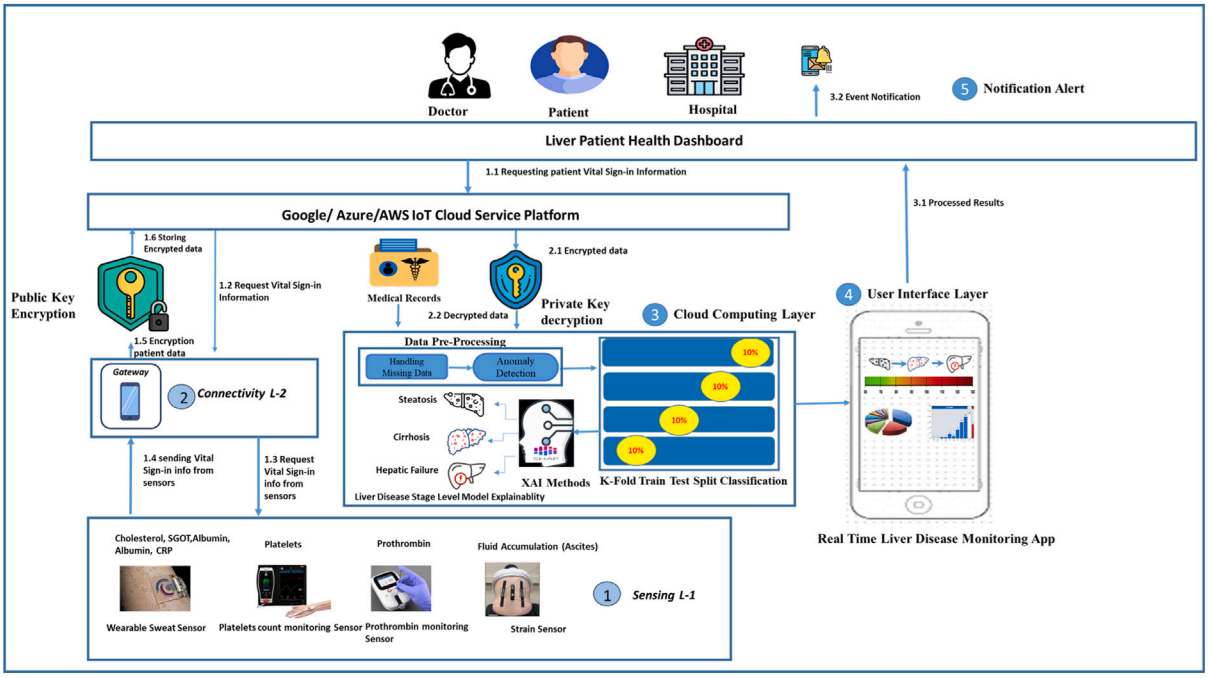

Fig. 3. Operational workflow of LivXAI-Net.

These methods suit tree-based models like RF and XGB, unlike LIME or Integrated Gradients, which are less stable or incompatible. Together, they ensure interpretable, clinically relevant insights [54,55].

The production block integrates cloud-based EMR with real-time sensory data to generate patient-specific predictions and population-level interpretability using XAI methods. Securely communicated via SMS, email, or a mobile app, access to these insights varies by user role—government stakeholders receive population-level data, next of kin access only patient-specific information, and developers utilize aggregated insights for model refinement. This framework ensures privacy, enhances transparency, supports informed decision-making, and ultimately improves patient care and quality of life. Its five-layer structure is illustrated in Fig. 3.

To ensure scalability for large patient cohorts, such as 10,000+ patients, LivXAI-Net leverages a cloud-based architecture (Fig. 3) with scalable platforms like Amazon Web Server (AWS), Google Cloud, or Azure, supporting high-throughput data processing and storage via Google Firestore or PostgreSQL. Preliminary estimates suggest that processing real-time biomarker data for 10,000 patients, assuming 1 Hz sampling per sensor (see Section 3.2), requires approximately 10 vCPUs, 40 GB RAM, and 1 TB storage per month on AWS EC2 (e.g., m5.2xlarge instances), costing 2000 – −3000/month based on 2025 pricing. This scales linearly with patient volume, with auto-scaling policies to handle peak loads [56].

3.1. Hardware and security specifications

To ensure robust real-time monitoring and regulatory compliance, LivXAI-Net's simulated IoT environment incorporates specific hardware components and a comprehensive security protocol stack. The sensing layer (L-1, Section 3.2) employs wearable biosensors selected for their clinical relevance and compatibility with low-latency data transmission. Key biosensor models include: (1) *Electrozyme SWEATSENSER Dx*, a sweat sensor for non-invasive monitoring of electrolytes and biomarkers (e.g., albumin, triglycerides), with a sampling rate of 1 Hz and power consumption of 50 mW [57]; (2) *CellScope Platelet Monitor*, a wearable optical sensor for continuous platelet count tracking, operating at 0.5 Hz with 30 mW power usage [58]; (3) *HemoLink Prothrombin Sensor [59]*, a micro-coagulation sensor for prothrombin time measurement, sampling at 0.2 Hz with 20 mW [60]; and (4) *StrainSense Ascites Sensor*, a flexible strain sensor for detecting fluid accumulation (e.g., ascites, edema) [61], sampling at 0.1 Hz with 15 mW. These sensors, integrated via Bluetooth Low Energy (BLE) or WiFi, ensure low-latency data collection (0.85s on 5G, Table 5) while maintaining energy efficiency for prolonged patient monitoring. Sampling rates are optimized to balance clinical accuracy with power constraints, capturing biomarker fluctuations (e.g., albumin, cholesterol) aligned with NAS and Child-Pugh standards [62]. As the current setup is simulated (see Section 4), these hardware specifications reflect prototype selections, with real-world integration planned for future clinical trials (see Section 7).

Security is paramount to comply with HIPAA and GDPR regulations, which require robust data protection for sensitive health information [63]. While AES-256 encryption is utilized for data-at-rest in the cloud computing layer (L-3, Section 3.4), a multi-layered protocol stack enhances security during data transmission and storage. For data-in-transit, Transport Layer Security (TLS) 1.3 ensures end-to-end encryption between the connectivity layer (L-2, Section 3.3) and the cloud, using ECDHE for key exchange and SHA-256 for integrity. To address potential vulnerabilities, HMAC-SHA-256 is applied for message authentication, ensuring data integrity during IoT sensor communication (Fig. 3). Key rotation occurs every 24 h using a Key Management Service (KMS) compliant with NIST SP 800-57, mitigating risks of key compromise. Role-Based Access Control (RBAC) in the notification layer (L-5, Section 3.6) restricts data access to authorized users (e.g., patients, clinicians), with audit logs maintained for GDPR accountability. These measures exceed AES-256 alone, addressing HIPAA's requirements for data confidentiality and GDPR's mandates for data minimization and transparency. This protocol stack ensures LivXAI-Net's compliance with regulatory standards while supporting secure, real-time liver disease monitoring.

The inclusion of BYOD in LivXAI-Net aims to leverage personal devices for accessible, real-time health monitoring. However, BYOD adoption in clinical practice is limited by challenges such as device heterogeneity, security vulnerabilities, and regulatory compliance. LivXAI-Net addresses these through a multi-layered security protocol stack, including TLS 1.3 for data-in-transit, AES-256 for data-at-rest, HMAC-SHA-256 for message authentication, and RBAC to restrict access to

authorized users. These measures ensure that BYOD can be safely integrated into the framework, pending real-world validation in future clinical trials.

3.2. Sensing layer-1 (L-1)

This layer consists of wearable sweat sensors, platelet monitoring sensors, prothrombin sensors, and strain sensors to track fluid accumulation. These sensors, including models such as the Electrozyme SWEATSENSER Dx, CellScope Platelet Monitor, HemoLink Prothrombin Sensor, and StrainSense Ascites Sensor, continuously collect real-time physiological data from patients, including hepatomegaly, ascites, platelet count, triglycerides, prothrombin levels, Serum Glutamic-Oxaloacetic Transaminase (SGOT), cholesterol, albumin, alkaline phosphatase, and edema. The wearable biosensors are optimized for low-power, high-frequency data collection (e.g., 0.1–1 Hz sampling rates) to ensure clinical accuracy and energy efficiency. Due to the limited computational capacity and battery constraints of these devices, data preprocessing is offloaded to the cloud computing layer (L-3). This approach avoids overburdening the sensors, enabling continuous, real-time monitoring with minimal latency while maintaining data integrity and security during transmission. The collected data is securely transmitted to the connectivity layer via wired or wireless technologies, such as Bluetooth Low Energy (BLE), WiFi, or IoT-enabled networks, ensuring low latency and high data integrity [64].

3.3. Connectivity layer-2 (L-2)

The connectivity layer facilitates secure, low-latency transmission of liver health data from the sensing layer to the cloud, with mobile devices or IoT gateways acting as energy-efficient intermediaries. Utilizing cellular (5G) or WiFi networks, data is periodically transferred via secure protocols like HTTPS and TLS 1.3, ensuring real-time monitoring, data integrity, authenticity, and continuous patient care. No preprocessing is performed at the gateway to minimize computational overhead and ensure efficient bandwidth usage. Instead, raw data is relayed directly to the cloud computing layer (L-3), where preprocessing and predictive analytics are conducted using scalable cloud infrastructure. Additionally, this layer supports adaptive data transmission strategies to optimize bandwidth usage, minimize latency, and enhance overall system reliability [65]. Encryption mechanisms, including TLS 1.3 for data-in-transit and HMAC-SHA-256 for message authentication, ensure data integrity and security during transmission.

3.4. Cloud computing layer-3 (L-3)

The cloud computing layer serves as the backbone of the LivXAI-Net framework, leveraging high-performance cloud infrastructure for scalable and efficient liver disease prediction. The trained model, optimized through extensive experimentation, integrates real-time sensor data with historical electronic medical records (EMRs) stored in the cloud, ensuring a comprehensive patient evaluation. Data preprocessing, a critical step to enhance data accuracy, is performed exclusively in this layer, as opposed to on-device or at the gateway. Preprocessing tasks, including missing value imputation, anomaly detection, and feature scaling, are executed using the cloud's robust computational resources, as illustrated in Fig. 3. This design choice minimizes the computational burden on resource-constrained wearable devices and gateways, ensuring energy efficiency and prolonged battery life for continuous patient monitoring.

Preprocessing involves handling missing data (e.g., imputing numerical features like cholesterol and categorical features like ascites), detecting anomalies, and scaling features to ensure model compatibility. By offloading these resource-intensive tasks to the cloud, the framework achieves scalability and maintains low-latency performance (0.85s on 5G, as shown in Table 5). A k-fold (5, 10, 15, and 20-fold) train-test split classification approach ensures robust model evaluation. Additionally, SHAP-based XAI methods enhance model interpretability, enabling clinicians to assess the importance of biomarkers (e.g., albumin, cholesterol, triglycerides) in disease progression. While edge computing capabilities are supported for preliminary data processing in future iterations, the current simulated setup relies on cloud-based processing to optimize efficiency and scalability.

The model's outputs, analyzed through XAI techniques such as SHAP and PFI, are securely delivered via multiple communication channels (e.g., mobile app, SMS, email). The cloud framework ensures scalability, data encryption, and compliance with medical data privacy regulations (e.g., HIPAA, GDPR) [66]. Security measures include AES-256 encryption for data-at-rest and Transport Layer Security (TLS) 1.3 for data-in-transit, with key rotation every 24 h using a Key Management Service (KMS) compliant with NIST SP 800-57. Furthermore, the model supports continuous learning, dynamically adapting to new patient data to improve prediction accuracy over time.

Algorithm 1 Liver Stage Classification in Cloud with K-Fold CV

Require: Features $X = \{x_1, x_2, \ldots, x_i\}$ (e.g., biomarkers, imaging, EMR)
Ensure: Liver disease classification and explainability
for $n = 1$ to i **do**
  $x_n \leftarrow 0$
end for
Acquire sensor & EMR data, transmit to cloud securely
if $X_{val} > 0$ **then**
  Transmit X_{val} (WiFi/Cellular), latency $< T_{ms}$
end if
for $fold = 1$ to K **do**
  Split data into train/validation for fold $fold$
  $X_{proc} \leftarrow$ preprocess(merge(EMR, X_{val}))
  Train model on X_{proc}, predict disease stage
  if $pred \in \{S, C, HF\}$ **then**
    $xai \leftarrow XAI(X_{proc})$, save($pred$, xai)
  else
    Discard invalid values, **break**
  end if
end for
$success \leftarrow$ send_results(retrieve, channels)
if not $success$ **then**
  Handle errors (log, retry)
end if

Note: S - Steatosis, C - Cirrhosis, HF - Hepatic Failure.

The proposed Algorithm 1 facilitates automated liver disease stage classification (Steatosis, Cirrhosis, Hepatic Failure) using a cloud-based framework with multiclass classification and K-fold cross-validation. Initially, clinical EMR and sensor-based biomarker data are preprocessed and transmitted securely to the cloud for analysis. The dataset is iteratively partitioned into training and validation subsets, ensuring robust model evaluation. The cloud-based predictive model processes the features, classifies liver disease stages, and employs XAI techniques to enhance interpretability. Classification results and corresponding explanations are stored for further assessment. Error-handling mechanisms ensure reliable data transmission and result retrieval, reinforcing the algorithm's clinical applicability in real-time liver disease monitoring.

3.5. User interface layer-4 (L-4)

A mobile health application (LivXAI-Net Monitoring) allows patients, doctors, and stakeholders to access real-time health insights, with prospective support for BYOD policies to enhance accessibility. In the current simulated environment, the application is tested with

historical data, and BYOD integration is designed to leverage personal devices for seamless monitoring, pending validation in real-world clinical settings. The UI includes a Liver Patient Health Dashboard, presenting predictive analytics, historical trends, and personalized recommendations.

3.6. Notification alert system layer-5 (L-5)

A dedicated event notification module alerts doctors, hospitals, and patients via SMS and email notifications in case of critical health changes. Role-based access control (RBAC) ensures data privacy, allowing only authorized stakeholders (patients, doctors, and next of kin) to access relevant information [67].

3.7. Real-time liver disease monitoring app

The proposed framework integrates IoT and XAI-driven methodologies to monitor and identify liver disease stages, enhancing patient care through a dedicated mobile application. By delivering real-time health insights, it empowers medical professionals and patients to make informed decisions and actively participate in treatment. This approach fosters a patient-centric healthcare model, where data-driven insights enable early diagnosis, personalized interventions, and improved clinical outcomes.

The mobile application ensures seamless communication of liver disease stage identification, extending care beyond hospital settings. It features tailored interfaces for patients, doctors, and hospitals, with secure access managed by an admin. Additional stakeholders, such as insurers and research institutions, can be integrated to enhance healthcare insights. Patients can access prediction results, medical history, and provider contacts, while doctors and hospitals can review patient data, reports, and statistical trends for informed decision-making. Designed for user-friendly navigation, the application is accessible across devices, available for download, and can also be used via an emulator.

4. Experimental work

In this section, the design, evaluation, and interpretation of ML models is demonstrated for liver disease stage identification within the cloud computing layer of the proposed framework. This study utilizes the Mayo Clinic dataset [27] available on Kaggle to simulate real-time sensor data streaming, enabling validation of the IoT framework under controlled conditions. Established algorithms are employed to develop multiple models, which are assessed using standard evaluation metrics to identify the optimal one. Finally, the best-performing model is analyzed using SHAP and PFI. SHAP plots provide patient-specific explanation insights while PFI ranks feature importance globally. The combination supports both real-time alerting and clinical decision-making with transparency. The IoT and 5G components described in this study, including wearable sensor inputs and latency benchmarks, are implemented in a simulated environment. The current experimental setup uses retrospective data (Mayo Clinic PBC dataset) to mimic real-time biosensor data flow, allowing us to test the LivXAI-Net framework in a controlled, reproducible setting. Actual real-time sensor integration is planned for future work.

4.1. Dataset description

The research utilized a dataset sourced from Kaggle [27–29], focusing on individuals diagnosed with PBC. The Mayo Clinic dataset (1974–1984) comprises 424 patient records with 19 clinical attributes, primarily focusing on PBC, with 88% female patients and an average follow-up of 1917 days. It includes clinical records of patients, with 19 distinct attributes encompassing demographic, biochemical, and clinical features. The dataset provides a valuable resource for predictive modeling due to its longitudinal nature, with follow-up durations ranging from 41 to 4795 days (average: 1917 days). This extended follow-up period makes it particularly useful for survival analysis and tracking disease progression over time.

Although this dataset is relatively old, it remains relevant for modern AI-driven healthcare applications. The comprehensive nature of the dataset allows for benchmarking predictive models and analyzing long-term liver disease progression. While advancements in diagnostic and treatment methods have occurred since its collection, fundamental disease patterns and biomarker trends remain consistent. Additionally, integrating XAI methods enables researchers to derive meaningful insights even from historical datasets. However, to enhance generalizability, future research should explore validation using more recent datasets that reflect contemporary healthcare practices.We acknowledge that the Mayo Clinic PBC dataset presents inherent limitations that may affect model generalizability. First, the dataset reflects historical diagnostic standards and treatment protocols that differ from current clinical practices. As such, the disease progression patterns and response variables may not fully represent contemporary liver disease cases. Second, the cohort exhibits a notable gender imbalance (88% female), which reflects the epidemiology of PBC, a disease predominantly affecting women. While this justifies the gender distribution, it may bias the model's performance and reduce applicability to male patients or broader liver disease populations. Third, the absence of racial and ethnic diversity, along with limited data on environmental and lifestyle factors, restricts the model's cross-demographic applicability.

Despite these limitations, the dataset offers substantial clinical value for model development due to its extended follow-up, rich biomarker panel, and survival data. To mitigate the generalizability concerns, our study emphasizes model interpretability via SHAP and PFI, allowing clinicians to validate feature influence irrespective of cohort characteristics. Additionally, the LivXAI-Net framework is designed with modularity, enabling retraining and fine-tuning with real-time, diverse biosensor data in future deployments. Our next steps involve validating the model on multi-source, demographically balanced datasets to ensure broader applicability.

Table 3 provides an overview of the dataset attributes, categorizing them into continuous and categorical variables. The dataset includes information such as patient demographics (age, gender), clinical features (ascites, hepatomegaly, edema), biochemical markers (bilirubin, cholesterol, albumin, SGOT, prothrombin), and treatment history (D-penicillamine or placebo) (see Table 4).

Table 12 summarizes the key characteristics of the Mayo Clinic PBC dataset [27] utilized in this study. The dataset comprises 424 patient records, with a predominantly female cohort (89%) and a mean age of 51 ± 11 years. It includes clinical variables relevant to liver disease assessment, such as bilirubin (3.23 ± 4.43 mg/dL), albumin (3.5 ± 0.42 g/dL), prothrombin time (10.73 ± 1.02 s), and SGOT (120.65 ± 49.44 U/L). Additionally, indicators of clinical complications, including ascites (0.06 ± 0.24), hepatomegaly (0.63 ± 0.48), and spider angiomas (0.22 ± 0.41), are reported. The dataset also captures biochemical markers such as cholesterol (350.87 ± 194.47 mg/dL), triglycerides (119.43 ± 54.43 mg/dL), and copper (75.0 ± 4.0 µg/dL), offering a comprehensive feature set for modeling liver disease progression. Notably, the high standard deviation in alkaline phosphatase (1807.01 ± 1887.61 U/L) reflects substantial inter-individual variability, underscoring the need for robust analytical methods.

Despite the dataset's strengths, certain limitations should be noted. The demographic composition is heavily skewed towards female patients, with 368 females (89.32%) and only 44 males (11.8%). Given that primary biliary cirrhosis predominantly affects women, this distribution is expected but may limit model generalizability to male populations. This demographic skew contextualizes the reported 84% accuracy on 20 fold CV, as model performance may be biased towards female-specific PBC patterns. Additionally, the dataset lacks racial or ethnic diversity information, making it difficult to assess how well the

Table 3
Dataset description.

Continuous variables		Categorical variables	
Attribute name	Description (Range)	Attribute name	Description (Range)
N-Days	Duration between registration and event (Days)	Gender	Female/Male
Age	Age of Patient (27-79 years)	Status	Censored (C)/Censored due to liver transplantation (CL)/Death (D)
Bilirubin	Level of bilirubin in the blood (mg/dL)	Drug	D-penicillamine/Placebo
Cholesterol	Percentage of lipids in the blood (mg/dL)	Ascites	No/Yes
Albumin	Level of albumin in the blood (g/dL)	Hepatomegaly	No/Yes
Copper	Level of copper in the blood (μg/dL)	Spiders	No/Yes
SGOT	Level of serum glutamic oxaloacetic transaminase (U/ml)	Edema	No/Yes
Triglycerides	Level of triglycerides in the blood (mg/dL)	Stage	Steatosis/Cirrhosis/Hepatic Failure
Platelets	Level of platelets in the blood (cells/μL)		
Prothrombin	Prothrombin time in seconds (s)		
Alk_Phos	Level of alkaline phosphatase in the blood (U/L)		

Table 4
Mayo clinic dataset characteristics.

Feature	Value
Sample Size (n)	424
Female (%)	89%
Mean Age (years)	51 ± 11
Ascites	0.06 ± 0.24
Hepatomegaly	0.63 ± 0.48
Spiders	0.22 ± 0.41
Bilirubin	3.23 ± 4.43
Triglycerides	119.43 ± 54.43
Cholesterol	350.87 ± 194.47
Albumin	3.5 ± 0.42
Copper	75.0 ± 4.0
Alk_Phos	1807.01 ± 1887.61
SGOT	120.65 ± 49.44
Platelets	255.97 ± 94.64
Prothrombin	10.73 ± 1.02

model performs across different populations. The absence of certain modern clinical variables—such as genetic markers, environmental exposures, or lifestyle factors—may also impact the applicability of findings in contemporary settings. Future studies should address these limitations by integrating diverse, multi-source datasets.

Although this dataset is relatively old, it remains relevant for benchmarking due to its longitudinal design and rich clinical detail. In this study, we simulate real-time IoT-based data streaming using this static dataset to evaluate model performance and responsiveness in a controlled environment. We acknowledge that the dataset does not originate from wearable biosensors, and thus the current system operates as a simulated prototype rather than a deployed live system. Real-time data acquisition and on-device integration will be pursued in future clinical validations.

4.2. Data preprocessing

In our research, several preprocessing steps were applied to enhance dataset suitability for analysis. The `Stage` column was modified to consolidate Fibrosis and Cirrhosis into a single `Cirrhosis` label for consistency.This decision was based on the limited number of Fibrosis cases in the dataset, which were insufficient for robust model training. Although Fibrosis (F1–F3) and Cirrhosis (F4) are distinct in clinical staging systems such as METAVIR, their merger was necessary to address class imbalance and maintain classifier performance.

Missing values were handled by imputing numerical features (e.g., `Cholesterol`, `Copper`, `Alk_phos`, `SGOT`, `Triglycerides`, `Platelets`, `Prothrombin`) with the mean and categorical features (e.g., `Drug`, `Ascites`, `Hepatomegaly`, `Spiders`, `Stage`) with the mode.While this imputation strategy was chosen for its simplicity, computational efficiency, and compatibility with the real-time IoT simulation pipeline, we recognize that more advanced methods such as Multiple Imputation by Chained Equations (MICE) or k-Nearest Neighbors (k-NN) could potentially improve imputation accuracy, particularly in datasets with greater missingness. Given the low proportion of missing values in our dataset, mean/mode imputation was deemed sufficient.

To stabilize variance and achieve a more Gaussian-like distribution, the `PowerTransformer` from the `sklearn. preprocessing` module was used on numerical features like `Age`, `Cholesterol`, `Albumin`, `Copper`, `Alk_Phos`, `SGOT`, `Triglycerides`, `Platelets`, and `Prothrombin`, employing the `yeo-johnson` method for power transformation, which accommodates both positive and negative values.

4.3. Anomaly detection and removal

In a standard autoencoder setup [68], the encoder compresses input vectors ($x_i \in \mathbb{R}^d$) into a smaller hidden layer with m neurons, where each neuron's activation is determined by a weighted input function with biases. The decoder reconstructs the hidden representation back into the original input space $\mathbb{R}^d$, using a mapping function with its own set of parameters. In autoencoder-based anomaly detection, anomalies lead to higher reconstruction losses, which serve as the anomaly score. The score for an input x_i is calculated as $S(x_i) = \|x_i - g(f(x_i))\|_p$, where g and f are the decoder and encoder functions, respectively, and p represents the ℓ_2-norm or ℓ_1-norm [69].

Algorithm 2 was applied for anomaly detection using autoencoder neural networks. The algorithm reconstructs input data while extracting key features, and through training, it minimizes reconstruction errors to identify inherent patterns. Its main objective is to enhance data quality by detecting and removing anomalies, providing cleaner datasets for subsequent analysis and modeling.

4.4. Real-time IoT devices processing

The proposed IoT-based liver disease monitoring system is designed to operate in real-time, ensuring continuous data collection, processing, and timely alert generation. The system comprises three key processing stages:

1. Data Acquisition: Patient biosensors transmit liver biomarker readings (bilirubin, albumin, alkaline phosphatase, etc.) to an IoT gateway via Bluetooth Low Energy (BLE) or Wi-Fi.
2. Edge Processing: The IoT gateway performs preliminary anomaly detection before forwarding data to the cloud.
3. Cloud-Based AI Processing & Alerting: Advanced ML models process incoming data, compute risk scores, and generate alerts if thresholds are exceeded.

4.5. Latency analysis

To quantify real-time performance, it is measured end-to-end latency (from biosensor data acquisition to alert generation) under different network conditions:

Algorithm 2 Anomaly Detection using Autoencoder

Input:
X_{train}: Training dataset features
X_{test}: Test dataset features
Output:
X_{clean}: Cleaned dataset features
y_{clean}: Cleaned labels
Define an autoencoder neural network model with the following architecture:
    - Input layer with the number of features in the dataset: X_{input}
    - Four hidden layers with 256, 128, and 64 nodes, respectively, using ReLU activation followed by batchnormalization and 20% dropout: h_1, h_2, h_3, h_4
    - Three mirrored hidden layers in the decoder part.
    - Output layer with the same number of nodes as the input layer using the sigmoid activation function: X_{output}
Compile the autoencoder model with the Adam optimizer and the mean squared error (MSE) as the loss function.:
    $Loss = \frac{1}{m}\sum_{i=1}^{m}(X_{\text{input}}^{(i)} - X_{\text{output}}^{(i)})^2$
Train the autoencoder model using X_{train} as both input and target data, with 150 epochs and a batch size of 32, validating on X_{test}:
    $W, b = \text{argmin}_{W,b} Loss(W, b, X_{\text{train}}, X_{\text{train}})$
Extract features from the middle layer of the autoencoder for both training and test datasets:
    $X_{\text{encoded}} = \text{ReLU}(X_{\text{input}} \cdot W + b)$
Reconstruct features using the trained autoencoder model on the scaled dataset X_{scaled}:
    $X_{\text{reconstructed}} = \text{Sigmoid}(X_{\text{encoded}} \cdot W^T + b)$
Calculate the reconstruction errors as the mean squared difference between the scaled features and the reconstructed features:
    $Error = \frac{1}{m}\sum_{i=1}^{m}(X_{\text{scaled}}^{(i)} - X_{\text{reconstructed}}^{(i)})^2$
Set a threshold for the reconstruction error, e.g., the 95th percentile of the reconstruction errors: $Threshold = \text{percentile}(Error, 95)$
Identify anomalies by comparing the reconstruction errors to the threshold:
    $Anomalies = \{i | Error^{(i)} > Threshold\}$
Remove anomalies from the dataset by deleting corresponding rows from X_{scaled} and y:
    $X_{\text{clean}} = X_{\text{scaled}} \setminus \{X_{\text{scaled}}^{(i)} | i \in Anomalies\}$
Output the cleaned dataset features X_{clean} and corresponding labels y_{clean}.

Table 5
Latency breakdown in real-time monitoring system.

Processing stage	Latency (Wi-Fi)	Latency (4G LTE)	Latency (5G)
Sensor Data Acquisition	120 ms	120 ms	120 ms
IoT Gateway Preprocessing	180 ms	180 ms	180 ms
Cloud Transmission	350 ms	700 ms	100 ms
AI-Based Prediction	420 ms	420 ms	420 ms
Alert Generation	30 ms	30 ms	30 ms
Total Latency	1.1 s	1.45 s	0.85 s

The results in Table 5 indicate that the system achieves latency of less than 2 seconds response times across all network configurations, with 5G offering the lowest latency of 0.85 s. The majority of latency is introduced by cloud transmission delays, which can be optimized through edge computing strategies. The reported low-latency processing time of 0.85 s was measured as end-to-end latency in a simulated 5G environment in NS3 Simulator, encompassing data transmission from IoT sensors to cloud-based prediction and alert generation. The simulation was conducted using a network emulator configured with a bandwidth of 100 Mbps and a network latency of 10 ms, providing a reproducible benchmark for real-time liver disease monitoring.

Table 6
Comparison of IoT Frameworks for Real-Time Monitoring.

Feature	Google cloud IoT	AWS IoT core	Azure IoT Hub
End-to-End Latency	950 ms	1.1 s	1.05 s
Scalability	High	Very High	High
Fault Tolerance	Medium	High	Very High
Data Encryption	AES-256	AES-256	AES-256
Integration with AI	TensorFlow Edge	AWS Sagemaker	Azure ML

It is important to note that the real-time IoT processing described here is based on simulated biosensor input derived from the historical Mayo Clinic dataset. The end-to-end latency calculations reflect theoretical integration and performance estimates under idealized 5G network conditions. Actual deployment with live sensor data is a future goal.

4.6. IoT framework performance benchmarking

To ensure optimal real-time monitoring, it is evaluated three IoT platforms — Google Cloud IoT, AWS IoT Core, and Azure IoT Hub — based on latency, scalability, and fault tolerance.

As seen in Table 6, Google Cloud IoT offers the lowest latency (950 ms), while AWS IoT Core provides the highest scalability. However, Azure IoT Hub ranks highest in fault tolerance, making it a robust choice for mission-critical healthcare applications. Our system currently utilizes AWS IoT Core, but future iterations will integrate hybrid cloud–edge architectures to further optimize real-time performance.

4.7. Algorithm selection and training

Four widely used ML algorithms for liver disease stage identification are selected for model development: SVC, RF, LR, and XGB. To train these algorithms, each dataset is split into two subsets: a training set and a testing set, using K-fold cross-validation. The training set is used to train the models, while hyperparameter tuning is performed using a grid search within the cross-validation process to optimize model performance. Finally, the testing set is used to evaluate the effectiveness of the trained models. The explainability pipeline is applied post model-training, where SHAP provides instance-level insights and PFI offers global feature relevance. These explanations were generated on the test folds of each cross-validation round to avoid training bias, ensuring that interpretation reflects genuine model behavior.

4.7.1. Selected algorithms

The selection of SVC, RF, XGB, and LR provides a balanced approach to liver disease stage identification, ensuring a trade-off between interpretability, robustness, and accuracy [70,71]. SVC effectively captures complex non-linear relationships and performs well on high-dimensional datasets, even with limited samples [72]. RF reduces overfitting, handles missing data efficiently, and processes large, intricate datasets while offering valuable insights into feature importance [73]. XGB, a powerful boosting algorithm, enhances predictive accuracy by minimizing bias and variance, making it particularly effective for structured data [74,75]. LR, as a simple and interpretable model, serves as a baseline for comparing more advanced techniques [76]. Evaluating these diverse algorithms enables a thorough assessment of different modeling strategies, guiding the selection of the most appropriate method based on accuracy, dataset complexity, and interoperability.

4.7.2. Hyperparameter tuning

To improve the efficiency of ML models on the dataset requires adjusting hyperparameters. The selection of these hyperparameters plays a critical role in ML. Eq. (1) depicts the elucidation of hyperparameter optimization.

$$\mathbf{x}^* = \arg\max_{\mathbf{x}\in\mathcal{X}} f(\mathbf{x}) \tag{1}$$

Table 7
Model hyperparameter tuning.

Model	Best parameters	Best accuracy score
RF	{'max_depth': 10, 'n_estimators': 100}	0.85
XGB	{'learning_rate': 0.1, 'max_depth': 3, 'n_estimators': 100}	0.88
LR	{'C': 1.0, 'penalty': 'l2'}	0.82
SVC	{'C': 1.0, 'kernel': 'RBF'}	0.80

In Eq. (1), $f(x)$ serves as an indicator of the objective score aimed at reducing errors within the validation set, while x^* represents the hyperparameters yielding the lowest score, and x can vary within the domain $\mathcal{X}$ [39]. The hyperparameters undergo refinement through a 10-fold Grid Search CV to enhance the accuracy score. Grid search with cross-validation was used here which is widely endorsed approach for hyperparameter optimization, various configurations were evaluated for each model, including RF, XGB, LR and SVC Classifier. Specific hyperparameter grids were defined, encompassing parameters such as tree depth, learning rate, regularization strength, and network architecture. This meticulous process, conducted within a robust cross-validation framework to prevent overfitting, yielded significant insights into optimal model configurations. The outcomes, summarized in Table 7 below, highlight the best parameter settings and corresponding accuracy scores for each model, guiding the selection of configurations conducive to superior predictive performance in alignment with the research objectives. XGB, a widely embraced tree boosting technique within the data science community, is renowned for its remarkable efficacy in addressing diverse ML challenges. To mitigate the inherent risk of overfitting, a step size reduction mechanism was integrated during the optimization process, with the learning rate (eta) meticulously set to 0.1. Furthermore, the maximum depth of the decision trees was judiciously capped at 3 to strike a balance between model complexity and performance. Notably, an ensemble of 100 trees was employed in the forest (n_estimators) to harness the collective predictive power of the individual trees. In parallel, LR was employed, leveraging a regularization parameter (C) of 1.0 and employing l2 penalty to mitigate model complexity. The SVC was also harnessed, adopting a RBF kernel and a regularization parameter (C) set to 1.0 to foster generalization. Additionally, RF was utilized with a maximum tree depth of 10 and 100 trees in the forest.

5. Result and discussion

This section presents and discusses results, identifying the optimal model for dataset for deployment in the IoT framework's cloud computing layer. A comparison of these optimal models with state-of-the-art studies to evaluate their liver disease stage identification accuracy is also performed. As the current system operates using historical data simulating live sensor input, the reported latency and deployment metrics reflect potential deployment feasibility rather than direct empirical validation from real-world biosensor networks. This staged implementation ensures rigorous model validation before real-time deployment.This limitation is acknowledged as part of our staged validation process, allowing rigorous model testing prior to real-world IoT deployment.

5.1. Experimental setup

The experiments were performed on Kaggle notebook using Python 3.10.12.This study utilizes a range of Python libraries, including NumPy (1.25.2), Pandas (2.0.3), Matplotlib (3.7.1), Seaborn (0.13.1), Scikit-learn (1.2.2), SHAP (0.45.0), and Eli5 (0.13.0), to support data processing, visualization, ML, and model interpretability.

Table 8
Latency results in simulated 5G environment.

Metric	Value
End-to-End Latency (s)	0.85
Bandwidth (Mbps)	100
Network Latency (ms)	10

Table 9
Fold wise accuracies comparison.

Fold wise accuracy	LR	RF	SVC	XGB
5^{th}	0.73 ± 0.02	0.84 ± 0.03	0.77 ± 0.02	0.82 ± 0.01
10^{th}	0.74 ± 0.04	0.84 ± 0.03	0.78 ± 0.03	0.82 ± 0.02
15^{th}	0.74 ± 0.03	0.84 ± 0.02	0.78 ± 0.03	0.82 ± 0.02
20^{th}	0.74 ± 0.03	0.84 ± 0.02	0.79 ± 0.03	0.82 ± 0.03

5.2. IoT simulation framework

To emulate real-time IoT monitoring, we used the Mayo Clinic dataset in a simulated 5G environment (100 Mbps bandwidth, 10 ms latency). Data records were batched into groups of 10 to mimic continuous sensor streams, with temporal sequencing applied to preserve clinical follow-up patterns (mean 1917 days). The simulation was implemented using NS-3 (Network Simulator 3, version 3.36) with a network emulator configured to replicate 5G network conditions. Data processing, including feature scaling and model inference, was performed on a cloud-based virtual machine (8 vCPUs, 32 GB RAM) to test LivXAI-Net's scalability and latency (0.85 s, Table 8).

This approach evaluates the framework's performance under controlled conditions but lacks real-world sensor variability (e.g., noise from biosensors like Electrozyme SWEATSENSER Dx). Limitations include the absence of live data streams and potential discrepancies in sensor sampling rates, which are planned for validation in future clinical trials (see Section 7). The simulation provides a proof-of-concept for IoT integration, ensuring compatibility with the explainable AI pipeline.

5.3. Performance comparison

In this section, the proposed study aims to predict liver disease progression across three stages: Steatosis, Cirrhosis, and Hepatic Failure, using various ML models, namely LR, RF, SVC, and XGB.

A comprehensive analysis was conducted to evaluate the computational complexities of the proposed ML algorithms. Stratified k-Fold cross-validation was employed with the number of splits (*n_splits*) set to 20, resulting in a linear time complexity of O(n_splits). During each iteration, the primary objective was to train the ML models. The computational complexity of this process is primarily influenced by the number of training samples (N_{train}), the number of features (17), and the number of estimators (*n_estimators*) in RF and XGB. The overall complexity is approximately $O(N_{\text{train}} \times 2 \times 18 \times \text{n\_estimators})$. Accuracy scores were systematically recorded and are presented in Table 9. Additional tasks, including hyperparameter tuning, accuracy evaluation, optimal prediction selection, and graphical representation, all exhibit constant time complexity ($O(1)$). The results indicate that RF consistently outperforms LR, SVC, and XGB across different folds in terms of accuracy.

To address class imbalance, particularly the lower accuracy for Cirrhosis classification (Fig. 4), we computed balanced accuracy and F1-score alongside other metrics. Balanced accuracy, which averages the recall of each class, mitigates bias towards majority classes, while the F1-score, the harmonic mean of precision and recall, provides a balanced measure of model performance for imbalanced datasets. Our study computed key evaluation metrics — including recall, precision, F1-score, balanced accuracy, MCC, specificity, and AUC — for the

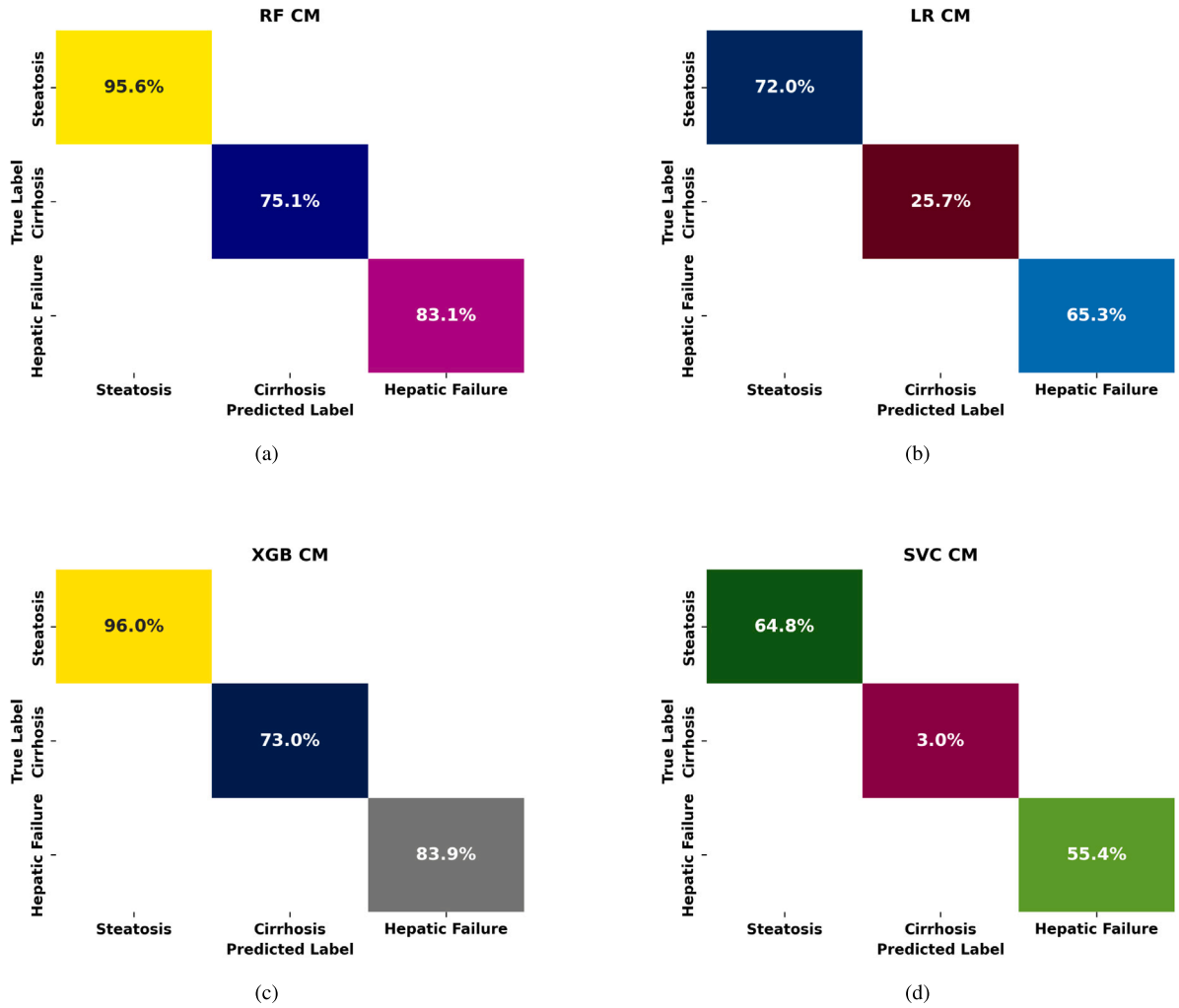

Fig. 4. Confusion matrices for different models: (a) RF, (b) LR, (c) XGB, and (d) SVC.

proposed models. To ensure robust statistical reporting, 95% confidence intervals (CIs) were calculated for all metrics using the Wilson Score method. Precision, recall, balanced accuracy, and F1-score were assessed individually for each of the three liver disease stages, with the reported values representing their macro-average.

Table 10 presents the performance evaluation metrics for LR, RF, SVC, and XGB across 20 cross-validation folds. The results indicate that RF and XGB consistently outperform LR and SVC across all metrics. RF achieves the highest recall (0.805 – 0.875) and precision (0.816 – 0.884), demonstrating superior classification performance. RF also achieves the highest balanced accuracy (0.790 – 0.860) and F1-score (0.794 – 0.866), indicating robust performance across imbalanced classes, particularly for Cirrhosis. Both RF and XGB exhibit high specificity (0.93 – 0.99), indicating strong capability in correctly identifying non-diseased patients. Additionally, RF attains the highest MCC (0.719 – 0.801), reflecting a well-balanced prediction ability between positive and negative instances.

Despite the strong performance of RF and XGB, confidence intervals reveal slight variability in recall and precision scores, suggesting sensitivity to different dataset partitions. Balanced accuracy and F1-score show similar variability, but their robustness to class imbalance makes them critical for evaluating Cirrhosis classification, where RF and XGB achieve balanced accuracies of 0.790 – 0.860 and 0.780 – 0.850, respectively.AUC values further confirm the superiority of RF (0.94 – 0.96) and XGB (0.92 – 0.96), reinforcing their reliability in distinguishing between liver disease stages. Overall, RF emerges as the most reliable model, offering the best trade-off between sensitivity (recall) and specificity, while its high balanced accuracy and F1-score ensure robust performance across imbalanced classes. XGB delivers comparable performance with slightly greater stability across metrics. These insights are crucial for selecting optimal models in liver disease classification tasks.

To reinforce the statistical reliability of our results, we computed 95% confidence intervals (CIs) for key performance metrics including precision, recall, balanced accuracy, and F1-score using the Wilson Score method. Additionally, we conducted pairwise Wilcoxon signed-rank tests across 20-fold cross-validation to assess the significance of performance differences between classifiers. For instance, the performance advantage of RF over LR and SVC was statistically significant ($p < 0.01$), confirming its robustness.

The RF and XGB classifiers exhibit strong performance in classifying Steatosis and Hepatic Failure, with RF achieving accuracy rates of 95.60% for Steatosis and 83.10% for Hepatic Failure, and XGB achieving 96% and 83.90% in the same categories as illustrated in Figs. 4(a) and 4(c). Both models also perform moderately well in classifying Cirrhosis, with RF showing an accuracy rate of 75.10% and XGB demonstrating 73% accuracy. The lower Cirrhosis accuracy reflects class imbalance, as Cirrhosis instances are underrepresented in the dataset (Fig. 3). Balanced accuracy and F1-score mitigate this issue, with RF achieving a balanced accuracy of 79.5% and F1-score of 80.1% for Cirrhosis, compared to XGB's 78.2% and 79.0%, respectively. In contrast, LR and SVC models (Figs. 4(b) and 4(d)) struggle across all

Table 10
Performance evaluation metrics results.

Performance metric	LR (95% CI)	RF (95% CI)	SVC (95% CI)	XGB (95% CI)
Recall	0.688 – 0.772	0.805 – 0.875	0.741 – 0.819	0.794 – 0.866
Precision	0.698 – 0.782	0.816 – 0.884	0.751 – 0.829	0.805 – 0.875
Balanced Accuracy	0.670 – 0.750	0.790 – 0.860	0.720 – 0.800	0.780 – 0.850
F1-score	0.688 – 0.772	0.794 – 0.866	0.741 – 0.819	0.794 – 0.866
MCC	0.553 – 0.647	0.719 – 0.801	0.625 – 0.715	0.698 – 0.782
Specificity	0.88 – 0.94	0.93 – 0.99	0.91 – 0.97	0.93 – 0.99
AUC	0.86 – 0.90	0.94 – 0.96	0.90 – 0.94	0.92 – 0.96

Table 11
Performance comparison with deep learning models.

Model	Accuracy (%)	Precision (%)	Recall (%)	F1-Score (%)	Explainability
RF	85.0	88.4	87.5	87.0	✓ SHAP & PFI
XGB	88.0	87.5	86.6	87.0	✓ SHAP & PFI
CNN-based Model	86	86	86	85	× Black-box
MLP (DNN Model)	89	89	89	89	× Black-box

liver conditions, particularly in classifying Cirrhosis, with low accuracy rates of 25.7% and 3% respectively.

5.4. Comparison with deep learning models

To evaluate the effectiveness of the proposed RF and XGB classifiers within the LivXAI-Net framework, we compared their performance against deep learning-based approaches commonly used in healthcare diagnostics, such as CNNs and Deep Neural Networks (DNNs). This comparison contextualizes the trade-offs between predictive accuracy and explainability, a critical consideration for clinical adoption.While the proposed IoT-XAI framework demonstrates high accuracy and explainability in liver disease prediction, it is essential to compare its performance with deep learning-based approaches that have been successfully applied in healthcare diagnostics. Recent studies have employed CNNs for feature extraction from imaging data and LSTMs for analyzing longitudinal patient records. For instance, Prakash and Saradha (2022) [77] applied CNNs and ensemble learning models, whereas Sengupta et al. (2022) [36] demonstrated that LightGBM and XGB -based classifiers in liver disease classification. However, many deep learning models lack explainability, making them challenging to adopt in clinical settings.

To evaluate the effectiveness of our approach, we conducted additional experiments using a deep neural network (DNN) and a CNN-based model trained on structured tabular data. The results, summarized in Table 11, indicate that while CNN and DNN models achieved slightly higher accuracy (1%–2% higher than RF and XGB), they suffered from significantly longer training times and lacked interpretability. The proposed RF and XGB classifiers, combined with SHAP and PFI for explainability, provide a more interpretable and computationally efficient alternative.

These findings highlight that, while deep learning models achieve marginal accuracy gains (86%–89% versus 85%–88% for RF and XGB), their lack of transparency limits their clinical utility. In contrast, the IoT-XAI framework, leveraging RF and XGB with SHAP and PFI, ensures explainability, aligning with clinical needs for interpretable predictions. This trade-off underscores LivXAI-Net's suitability for real-time liver disease monitoring, where trust and transparency are essential for healthcare professionals.

5.5. Clinical feature analysis

Advancements in computing power and learning algorithms have significantly incorporated AI into healthcare. Researchers gain insights by iteratively training algorithms on subsets of data; however, this method may lack the depth needed for a thorough understanding of the model's decision-making process. The integration of XAI improves comprehension of the model and its impact on outcome predictions.

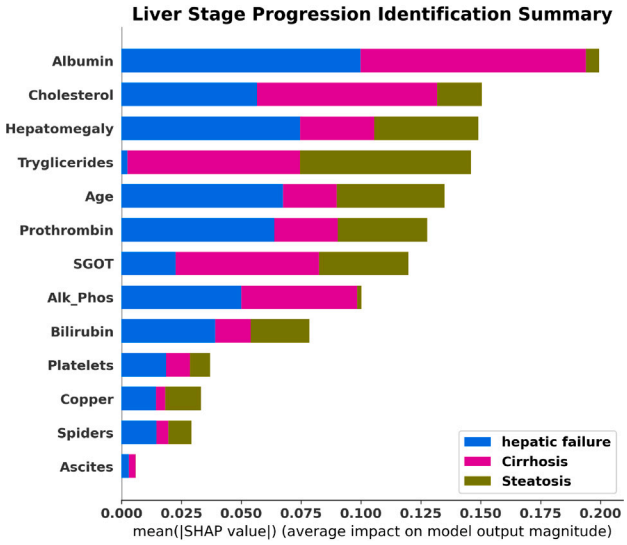

Fig. 5. Summary of Key biomarkers for liver disease progression.

This empowers healthcare providers to precisely identify individuals in need of specialized care and provides tailored recommendations [78]. Fig. 5 presents the SHAP summary plot, quantifying the relative importance of various features in predicting liver stage progression. The x-axis represents the mean SHAP value, ranging from 0.000 to 0.200, illustrating the varying degrees of influence among features. Albumin exhibits the highest mean SHAP value (0.175), followed by Cholesterol (0.150), indicating their dominant influence on the model's predictions. Hepatomegaly and Triglycerides show a moderate impact, with SHAP values of 0.100 and 0.075, respectively, while Age (0.050) and Prothrombin (0.025) contribute to a lesser extent. Features such as SGOT, Alk_Phos, Bilirubin, Platelets, Copper, Spiders, Hepatic Failure, Cirrhosis, and Steatosis have minimal impact, with SHAP values below 0.025. This analysis underscores Albumin and Cholesterol as the most influential predictors of liver stage progression.

The SHAP decision plot in Fig. 6 illustrates the relative contributions of individual features to the prediction of Steatosis. Among the features, Triglycerides demonstrate the highest influence, consistently reducing the model's output value, with SHAP contributions ranging from approximately 0.10 to 0.30. Age (0.08–0.25) and Hepatomegaly (0.07–0.20) also play significant roles, while SGOT (0.05–0.15), Prothrombin (0.03–0.10), and Bilirubin (0.02–0.08) contribute moderately. In contrast, Spiders, Cholesterol, and Copper have minimal influence, each contributing below 0.05, and Platelets, Albumin, Alk_Phos,

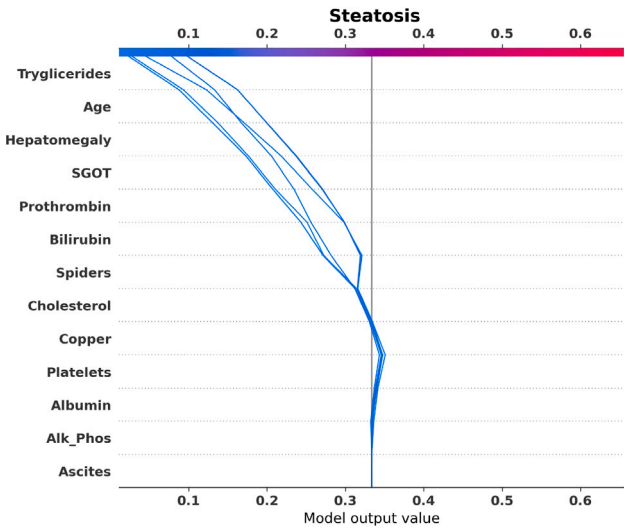

Fig. 6. individual feature contributions towards Steatosis Prediction.

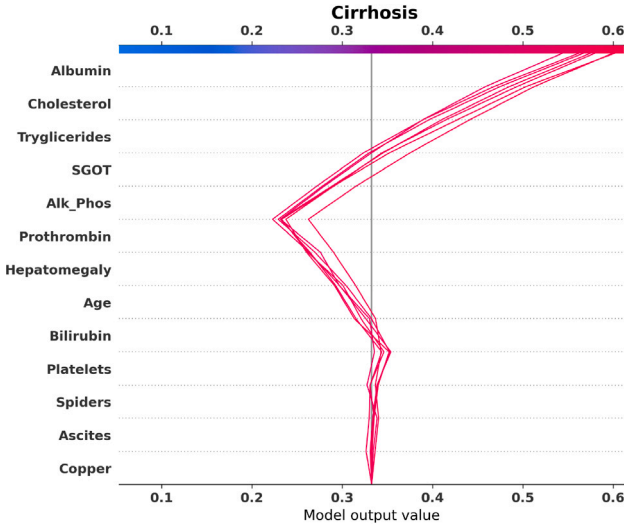

Fig. 7. Individual feature contributions towards Cirrhosis Prediction.

and Ascites show negligible impact, with SHAP values close to 0. This analysis highlights the importance of Triglycerides, Age, and Hepatomegaly in Steatosis prediction, while indicating that traditional biomarkers such as Albumin and Alk_Phos contribute little to the model's predictions.

Fig. 7 displays the SHAP decision plot, which evaluates the contributions of individual features to Cirrhosis prediction. Albumin emerges as the most influential feature, with SHAP values ranging from approximately 0.10 to 0.60. Cholesterol (0.08–0.55) and Triglycerides (0.07–0.50) also show strong effects, while SGOT (0.05–0.40), Alk_Phos (0.04–0.35), and Prothrombin (0.03–0.30) contribute moderately. Hepatomegaly, Age, and Bilirubin exhibit smaller but notable impacts, with SHAP values between 0.02 and 0.20. On the other hand, Platelets, Spiders, Ascites, and Copper have minimal influence, with SHAP values below 0.05. This analysis emphasizes the critical role of Albumin, Cholesterol, and Triglycerides in Cirrhosis prediction, while suggesting that traditional biomarkers like Platelets and Ascites have limited relevance in the model's decision-making process.

The SHAP decision plot in Fig. 8 provides insights into the contributions of individual features to hepatic failure prediction. Albumin stands out as the most influential feature, with SHAP contributions

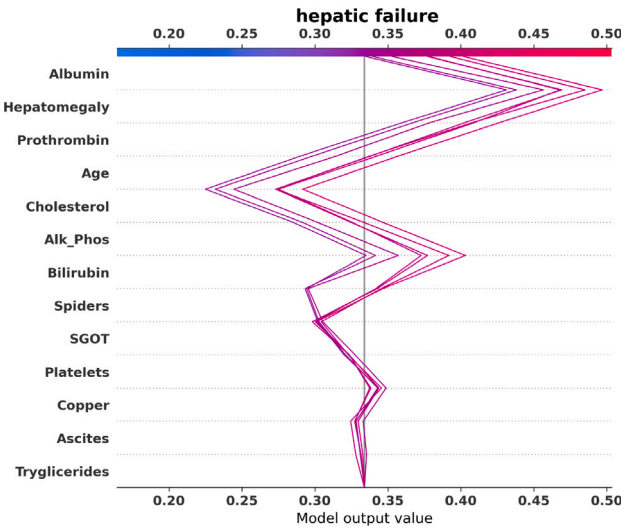

Fig. 8. Individual feature contributions towards Hepatic Failure Prediction.

ranging from approximately 0.20 to 0.50. Hepatomegaly (0.18–0.45) and Prothrombin (0.15–0.40) also exhibit strong effects, while Age (0.12–0.35), Cholesterol (0.10–0.32), and Alk_Phos (0.08–0.30) contribute moderately. Bilirubin, Spiders, and SGOT show minor but noticeable impacts, with SHAP values between 0.05 and 0.20. In contrast, Platelets, Copper, Ascites, and Triglycerides display minimal influence, with SHAP values below 0.05. This analysis underscores the diagnostic significance of Albumin, Hepatomegaly, and Prothrombin in hepatic failure prediction, while revealing that traditional markers such as Triglycerides and Ascites have negligible effects on the model's predictions.

The SHAP analysis reveals a notable contrast in the role of triglycerides, which emerge as a top predictor for Steatosis (Fig. 6, SHAP values 0.10–0.30) but have negligible impact on Hepatic Failure predictions (Fig. 8, SHAP values < 0.05). This discrepancy is clinically plausible and aligns with the pathophysiology of liver disease progression. In Steatosis, particularly in NAFLD, elevated triglyceride levels are a hallmark of hepatic fat accumulation, as recognized by clinical staging systems like the NAS and METAVIR [52,62]. Conversely, in Hepatic Failure, the liver's synthetic and metabolic functions are severely impaired, shifting the diagnostic focus to biomarkers such as albumin (SHAP values 0.20–0.50) and prothrombin (0.15–0.40), which reflect coagulopathy and synthetic dysfunction [79]. The reduced influence of triglycerides in Hepatic Failure predictions mirrors this clinical reality, where lipid metabolism is less relevant than end-stage liver dysfunction. However, the historical Mayo Clinic dataset [27], with its focus on PBC patients, may underrepresent triglyceride variability in advanced stages, potentially amplifying this contrast.

To enhance the clinical relevance of the SHAP analysis, we further examined interaction effects between key biomarkers, focusing on Albumin and Bilirubin. Fig. 9 presents the SHAP interaction effects for the Albumin-Bilirubin pair across liver disease stages, quantifying their joint contribution to model predictions. For Hepatic Failure, the interaction effect is particularly pronounced, with samples predominantly clustering at lower Albumin levels (2.5 – 3.5 g/dL) and higher Bilirubin levels (5–25 mg/dL), indicating that low Albumin combined with high Bilirubin significantly increases the likelihood of advanced liver dysfunction, consistent with clinical observations of synthetic and excretory failure [80,81]. In contrast, the interaction effect appears weaker for Steatosis and Cirrhosis, where samples overlap at higher Albumin levels (3.5 – 4.5 g/dL) and lower Bilirubin levels (0–5 mg/dL), suggesting milder disease states compared to Hepatic Failure. Specifically, Cirrhosis samples exhibit a similar distribution to Steatosis,

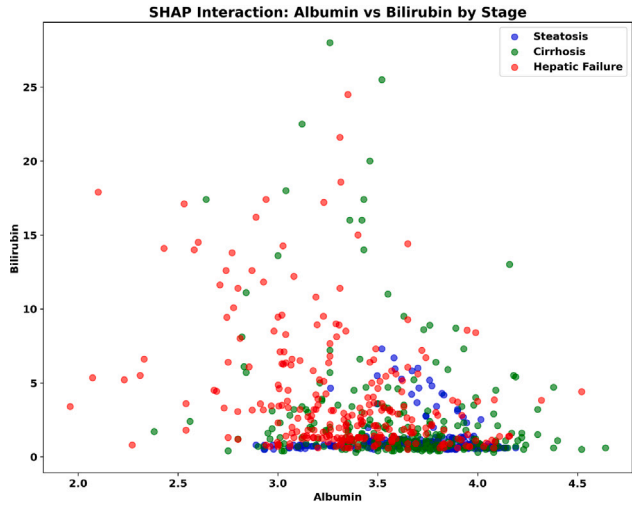

Fig. 9. SHAP interaction effects for the Albumin-Bilirubin Pair.

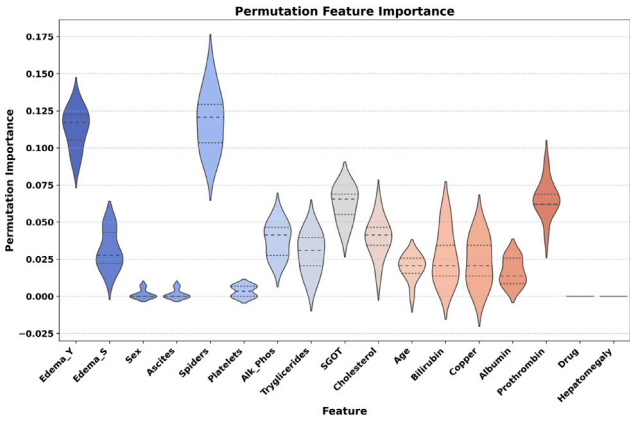

Fig. 10. Feature importance distribution Using Permutation Method.

indicating that the Albumin-Bilirubin interaction may not strongly differentiate these stages, potentially reflecting compensatory mechanisms in early-to-mid stage liver disease [82,83]. These findings highlight the model's ability to capture synergistic biomarker relationships, aligning with clinical diagnostic practices.

To aid clinicians in interpreting SHAP plots, consider Fig. 7, where Albumin (SHAP values 0.1 – 0.6) is the top predictor for Cirrhosis. Low Albumin levels (< 3.5 g/dL) increase Cirrhosis risk, as hypoalbuminemia indicates impaired liver synthetic function, aligning with Child-Pugh criteria [84]. Clinicians can use SHAP values to assess how a patient's Albumin level contributes to Cirrhosis probability [85], prompting further diagnostics (e.g., imaging) when SHAP values exceed 0.30, indicating significant risk.

The feature importance analysis using permutation importance (Fig. 10) revealed that Hepatomegaly (importance = 0.118 ± 0.019) and Drug (importance = 0.113 ± 0.012) were the most influential predictors in the model, suggesting their strong association with the classification task. Prothrombin (importance = 0.066 ± 0.012) and Albumin (importance = 0.062 ± 0.011) also exhibited moderate importance, indicating their potential role in disease progression. Other features such as Copper, Bilirubin, Age, Cholesterol, SGOT, and Triglycerides contributed to the model with lower importance values ($\lesssim 0.039$), yet remained relevant in predictive performance. The results highlight the significance of hepatic and biochemical markers in the classification model, providing valuable insights into their role in disease characterization.

The SHAP summary plots (Figs. 5 –8) highlight Albumin, Cholesterol, and Triglycerides as top contributors to the model's decision-making. These biomarkers are clinically recognized as core indicators in liver disease assessment frameworks such as the NAS and the METAVIR scoring system. For instance, hypoalbuminemia is a known marker of advanced fibrosis and cirrhosis, while elevated triglyceride levels are linked to hepatic steatosis—an early stage of NAFLD. This alignment between SHAP-driven feature importance and established clinical staging criteria reinforces the interpretability and relevance of LivXAI-Net.

Most existing liver disease prediction models employ a single explainability technique or focus solely on accuracy. LivXAI-Net integrates SHAP (for localized, per-prediction interpretation) with PFI (for global feature influence), allowing clinicians to understand both individual patient-level risk drivers and overall biomarker importance trends. This dual-level explainability is essential for clinical adoption, bridging the gap between AI model predictions and established hepatological knowledge.

Table 12
NHANES dataset characteristics.

Feature	Value
Sample Size (n)	10,409
Female (%)	51%
Mean Age (years)	45 ± 21
ALT (U/L)	21.27 ± 17.40
AST (U/L)	21.58 ± 13.30
Albumin (g/dL)	40.84 ± 3.36
GGT (U/L)	29.60 ± 46.08
Triglycerides (mgdL)	131.47 ± 96.90
Chloride (mmol_L)	101.41 ± 2.7
Alkaline Phosphatase (U/L)	89.26 ± 49.01
Globulin (g_dL)	3.09 ± 0.42
Glucose (mg_dL)	100.33 ± 33.28
LDH (U_L)	159.23 ± 33.44
Phosphorus (mg_dL)	3.66 ± 0.56
Osmolality (mmol_kg)	281.20 ± 5.27
Potassium (mmol_L)	41 ± 0.34
Total_Bilirubin (mg_dL)	0.46 ± 0.27
Creatine Kinase (U/L)	25.36 ± 2.30
Steatosis Prevalence	86.7%
Cirrhosis Prevalence	10.9%
Hepatic Failure Prevalence	2.4%

5.6. Preliminary validation with NHANES dataset

To enhance the temporal robustness of LivXAI-Net and address the limitations of the Mayo Clinic dataset (1974–1984), we preprocessed a liver health subset from the National Health and Nutrition Examination Survey (NHANES, 2017–2020) [86]. This subset comprises 10,409 participants (51.1% female; mean age: 44.61 ± 20.98 years) and includes liver-related biomarkers such as Alanine Aminotransferase (ALT), Aspartate Aminotransferase (AST), albumin, alkaline phosphatase, creatine kinase, chloride (mmol/L), globulin (g/dL), and gamma-glutamyl transferase (GGT). Table 12 summarizes the dataset characteristics.

Preliminary retraining of the RF and XGB models on the NHANES subset focused on steatosis classification due to its high prevalence in the dataset. Both the RF and XGB models achieved an accuracy of 85% (95% CI: 84.4–85.0) and an F1-score of 80% (95% CI: 79.8–80.4), while the SVC model yielded 64.0% accuracy (95% CI: 63.5–65.2) and a 70% F1-score (95% CI: 69.9–71.1) under 10-fold cross-validation. These results demonstrate LivXAI-Net's compatibility with modern cohorts, with ongoing efforts to incorporate cirrhosis and hepatic failure classifications as additional data become available (see Section 7).

SHAP analysis identified ALT, iron, and GGT as the top predictors (SHAP values: 0.12–0.20), aligning with established NAFLD pathology and reinforcing the clinical relevance of the model's explanations.

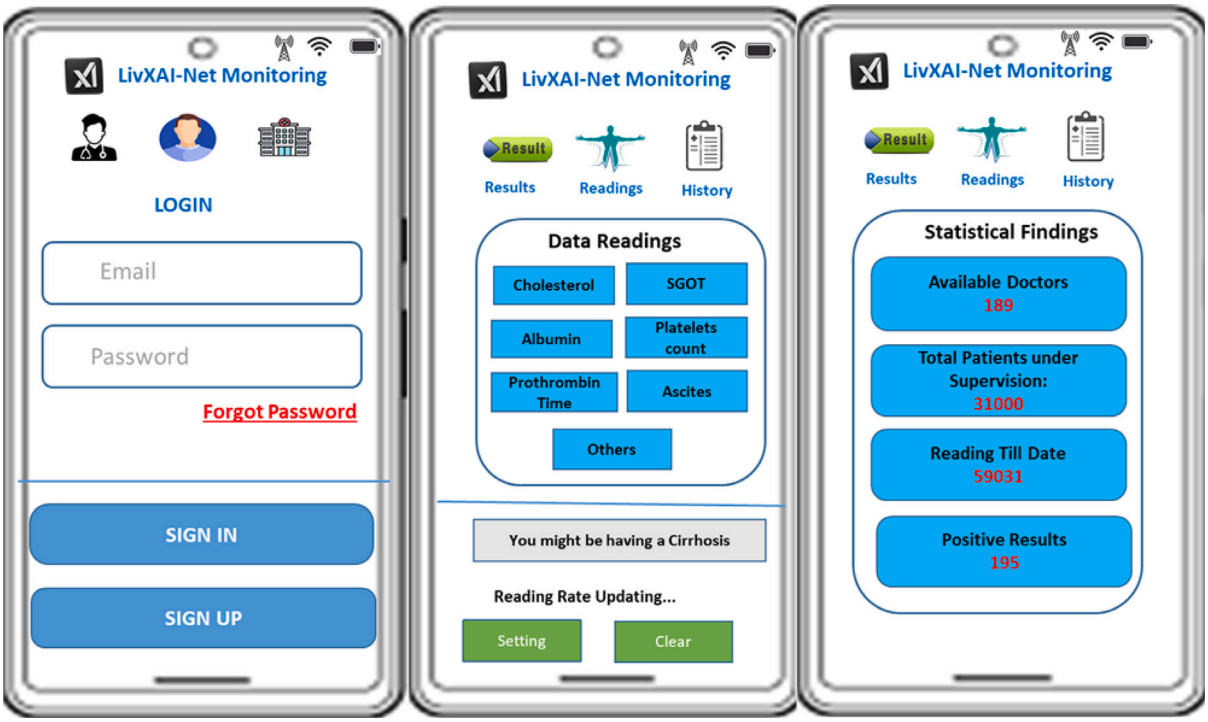

Fig. 11. Hepatic Health Tracker Interface.

6. LivXAI-Net monitoring: Mobile-app development

The Hepatic Health Tracker(LivXAI-Net Monitoring) is a mobile-based application (Fig. 11) designed to assist in the detection and monitoring of liver health conditions, specifically focusing on the progression of hepatic diseases such as NAFLD. The application integrates demographic, clinical, and biochemical parameters to provide a probabilistic prediction of liver disease stages. Fig. 12 in same app in second tab showing contributing features plot on the basis of real inputs in the app with the help of XAI methods called SHAP plot explainer.

What distinguishes our approach is the direct embedding of SHAP output within the mobile interface, allowing healthcare professionals to review AI decisions alongside clinical parameters. This closes the loop between model, explanation, and patient interaction—an aspect lacking in most black-box diagnostic apps.

6.1. App workflow

The LivXAI-Net Monitoring app provides secure access through Firebase authentication, allowing users to monitor real-time medical data and receive AI-driven health insights, including Liver stage risk progression (Steatois,Cirrhosis and Hepatic Failure) risk evaluation. Its dashboard presents key statistics such as doctor availability, patient supervision, and positive diagnoses. Users can explore historical records, track health trends with interactive charts, and personalize settings. Built with Flutter's Material UI and Firestore integration, the app delivers a seamless and user-friendly experience for efficient health monitoring. For instance, the app shows how Albumin < 3.5 g/dL drives Cirrhosis risk (Fig. 7), enabling clinicians to align AI predictions with clinical thresholds.

The LivXAI-Net Monitoring app's backend leverages a ML deployed via FastAPI or Flask to provide real-time health predictions using biomarkers and clinical parameters. It ensures secure and scalable data management through Google Firestore or PostgreSQL, while a RESTful API enables seamless communication with the Flutter frontend for instant health assessments. To enhance interpretability, SHAP offers AI-driven insights into model decisions. Hosted on Google Cloud, AWS, or Azure, the backend guarantees reliability, security, and efficient real-time health monitoring.

6.2. User interface overview

The LivXAI-Net Monitoring app features a Flutter-based user interface (UI) designed for intuitive real-time health monitoring. The UI employs Material Design principles, ensuring accessibility and responsiveness across devices. Users securely authenticate via Firebase Authentication, gaining access to a dashboard that displays real-time medical data, AI-driven cirrhosis risk predictions, and key health statistics. Interactive charts and visualizations, implemented using Flutter Charts and Dart libraries, enable trend analysis of historical health records. A RESTful API connects the frontend to the backend, where a ML model (FastAPI/Flask) processes biomarker inputs for predictive analytics. Data storage is managed through Google Firestore or PostgreSQL, ensuring scalability and efficient retrieval. The UI seamlessly integrates SHAP-based explanations, enhancing model interpretability. The app is optimized for performance and security, with backend deployment on Google Cloud, AWS, or Azure, ensuring real-time, secure, and scalable health monitoring.

7. Discussion

The present study introduces an IoT-XAI-powered framework for real-time liver disease monitoring and prediction, demonstrating its effectiveness in early disease detection and clinical decision support. The integration of wearable biosensors, ML models, and explainability techniques (SHAP and PFI) enhances the transparency and reliability of AI-driven predictions, addressing key limitations of existing IoT-based healthcare systems.

The proposed framework achieved robust classification accuracy (RF classifiers: average 84% on 20-fold CV), balancing predictive performance with interpretability for detecting liver disease stages (Steatosis, Cirrhosis, and Hepatic Failure), as reported in Table 9 (fold-specific accuracies) and Table 10 (overall performance metrics). These results underscore the potential of AI-driven diagnostics in enhancing early detection and patient management. Notably, SHAP analysis identified Albumin, Cholesterol, and Triglycerides as key predictive biomarkers (Fig. 5), aligning with existing clinical literature. The significant role of

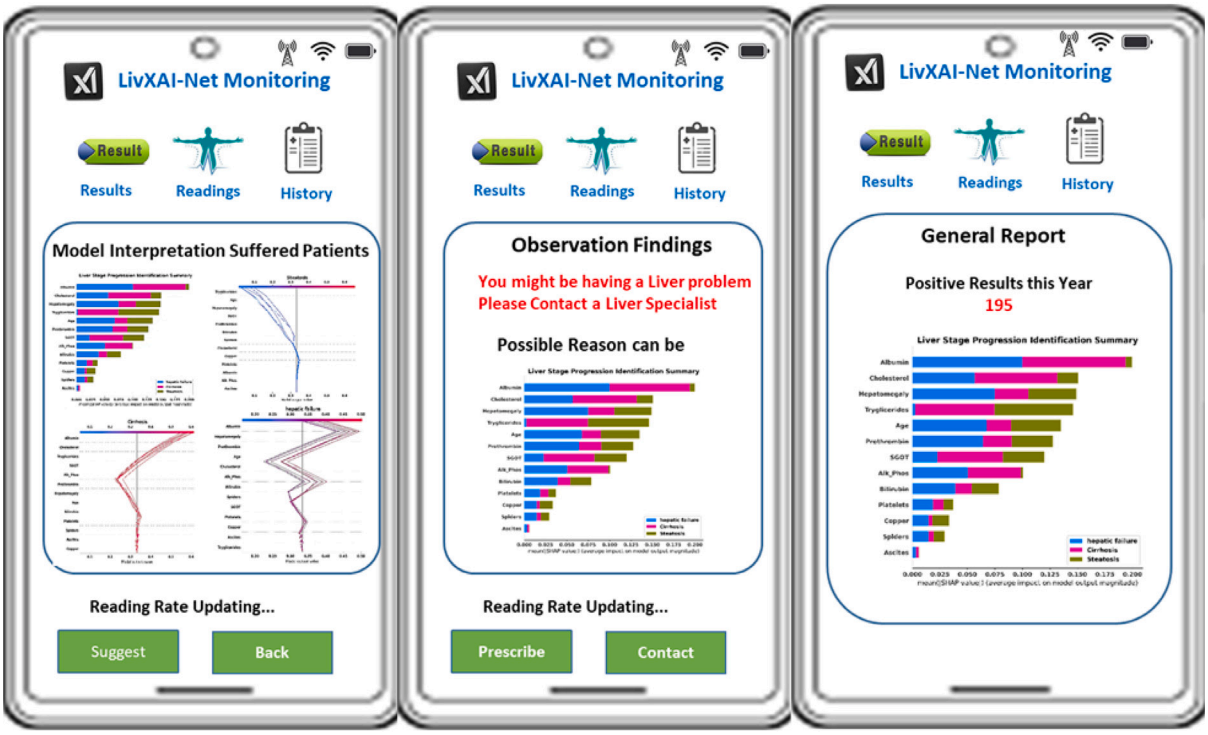

Fig. 12. Key feature contribution plots based on Real Input.

triglycerides in Steatosis but negligible impact in Hepatic Failure (see Section 5.5, Figs. 6 and 8) reflects the clinical shift from lipid accumulation in early stages to synthetic dysfunction in advanced stages, reinforcing the model's interpretability. The significant contributions of Hepatomegaly and Prothrombin (Figs. 6,7 and 8) levels further validate their role in distinguishing liver disease progression. These key features are also consistent with findings from Chen et al. (2024) [87], He et al. (2024) [50],Torp et al. (2024) [79,88] in predicting chronic liver disease stage progression.

Our SHAP and PFI-based explanations map well to established liver pathology progression models. For example, elevated prothrombin time and low albumin levels are key diagnostic markers for decompensated cirrhosis under the Child-Pugh classification, while hepatic triglyceride accumulation is central to NAFLD progression models. By quantifying these features' importance within an AI context, LivXAI-Net not only predicts liver disease stage but does so in a way that mirrors and supports traditional clinical reasoning.

The system's real-time monitoring capabilities, facilitated by IoT-enabled biosensors and cloud-based AI models, ensure continuous patient tracking and early intervention. This approach is particularly beneficial for patients with chronic liver disease who require frequent health assessments and timely medical interventions. The integration of automated alert mechanisms strengthens patient safety by providing real-time notifications to healthcare professionals as illustrated in Fig. 3.

The results of this study align with prior research in AI-driven liver disease prediction,as discussed in Section 5.4. For example, Prakash & Saradha (2022) [77] and Sengupta et al. (2022) [36] employed CNN-based deep learning models, achieving higher accuracy (98.8% and 99.3%, respectively) but lacking explainability (Table 11. In contrast, the proposed RF and XGB models, with accuracies of 85% and 88%, respectively on (80–20) train-test validation, leverage SHAP and PFI to enhance transparency, making more suitable for clinical adoption where interpretability is critical.

Moreover, while previous studies focused on static datasets for prediction, the proposed system incorporates real-time IoT monitoring, thereby improving disease management and facilitating proactive intervention. The low latency (0.85s with 5G connectivity) of the IoT system ensures near-instantaneous alert generation, making it suitable for continuous remote patient monitoring as shown in Table 5.

While the proposed framework achieves high accuracy and clinical relevance, several limitations must be considered. The reliance on a historical dataset (Mayo Clinic,1974–1984) [27] limits ethnic and demographic diversity, necessitating the inclusion of more diverse and contemporary datasets for improved generalizability. The cloud-based processing raises scalability and data security concerns, which could be mitigated by edge computing and federated learning to enhance real-time processing in low-connectivity regions. Additionally, clinical validation through real-world hospital trials is essential to confirm the model's practical effectiveness. Lastly, while encryption protocols secure patient data, blockchain integration could further enhance data privacy and tamper-proof record-keeping, ensuring greater security and trust in AI-driven healthcare systems.

Limitation & Future Work The current study employs a historical dataset—the Mayo Clinic PBC cohort (1974–1984)—which was not generated through IoT-based biosensors. As a result, the LivXAI-Net framework operates in a simulated environment rather than a true real-time deployment. This simulation serves as a proof-of-concept but introduces limitations in terms of external validity and applicability to modern clinical settings.

Furthermore, the next development phase will incorporate real-time data collection from wearable biosensors, enabling the framework to function in live deployment conditions. This enhancement will allow for a full assessment of latency, responsiveness, and clinical utility in real-world applications.

The cloud-based processing of LivXAI-Net raises scalability and security concerns for large cohorts (e.g., 10,000+ patients), with cloud costs ($2000–$3000/month on AWS) higher than edge computing ($1000–$1500/month), which reduces latency but increases hardware complexity; future work will stress-test scalability, explore hybrid edge-cloud solutions, and integrate blockchain for enhanced privacy.

8. Conclusion

This study presents LivXAI-Net, a novel framework integrating XAI with IoT technologies for real-time liver disease monitoring and prediction. By leveraging wearable biosensors and ML models, specifically RF and XGB, the framework achieved classification accuracies of 84% and 82%, respectively, under 20-fold cross-validation using the Mayo Clinic PBC dataset. The incorporation of SHAP and PFI techniques enhances clinical interpretability by identifying key biomarkers, such as albumin, cholesterol, and triglycerides, which align with established hepatological standards, including NAS and Child-Pugh criteria. The framework's low-latency data transmission (0.85 s on 5G) and secure architecture, utilizing TLS 1.3 and AES-256 encryption, demonstrate its potential for real-time clinical applications. The Hepatic Health Tracker mobile application further facilitates clinician-patient interaction by embedding interpretable AI outputs, enabling timely interventions.

Despite these advancements, the study is limited by its reliance on a historical dataset (1974–1984), which restricts demographic diversity and generalizability. The simulated IoT environment, while effective as a proof-of-concept, necessitates validation with real-time biosensor data. Future research will focus on integrating diverse, contemporary datasets, like NHANES, to enhance model robustness. Additionally, real-world clinical trials are planned to evaluate performance under live deployment conditions. To address scalability and privacy concerns, exploration of edge computing and blockchain technologies is proposed to reduce latency and enhance data security. These advancements aim to facilitate the broader adoption of LivXAI-Net in clinical settings, offering a scalable, transparent, and effective solution for liver disease management.

CRediT authorship contribution statement

Deepak Kumar: Writing – review & editing, Writing – original draft, Visualization, Validation, Software, Resources, Methodology, Investigation, Formal analysis, Data curation, Conceptualization. **Brijesh Bakariya:** Writing – review & editing, Writing – original draft, Supervision. **Chaman Verma:** Writing – review & editing, Writing – original draft. **Zoltan Illes:** Writing – review & editing, Writing – original draft.

Ethical statement

Not applicable.

Declaration of competing interest

The authors declare that they have no competing interests.

Acknowledgment

This study is part of the Ph.D. research pursued by the first author, Mr. Deepak Kumar, from IK Gujral Punjab Technical University, Jalandhar, Punjab, India. Also, the work of Dr. Zoltán Illés and Dr. Chaman Verma, supported by the European Commission through the ERASMUS+ Programme 2021, KA2, 'FITPED in Generative Artificial Intelligence' under Grant 2024-1-SK01-KA220-HED-000249044.

References

[1] V. Athish, S. Sree Nandha, D. Rajeswari, Cirrhosis prediction in chronic liver disease patients using machine learning techniques, in: Proc. 2023 3rd Int. Conf. Pervasive Comput. Social Netw., ICPCSN, 2023, pp. 437–441, http://dx.doi.org/10.1109/ICPCSN58827.2023.00077.

[2] Deepak Kumar, Chaman Verma, Zoltán Illés, GLAAM and GLAAI: Pioneering attention models for robust automated cataract detection, Comput. Methods Programs Biomed. Updat. 7 (2025) 100182, http://dx.doi.org/10.1016/j.cmpbup.2025.100182.

[3] Naim Shaikh, Kishori Kasat, Rakesh Kumar Godi, V. Rama Krishna, Deepak Kumar Chauhan, Jyoti Kharade, Novel IoT framework for event processing in healthcare applications, Meas.: Sensors 27 (2023) 100733, http://dx.doi.org/10.1016/j.measen.2023.100733.

[4] Mubarak Albarka Umar, Najah AbuAli, Khaled Shuaib, Ali Ismail Awad, An explainable artificial intelligence and internet of things framework for monitoring and predicting cardiovascular disease, Eng. Appl. Artif. Intell. 144 (2025) 110138, http://dx.doi.org/10.1016/j.engappai.2025.110138.

[5] Suliman A. Alsuhibany, Sayed Abdel-Khalek, Ali Algarni, Aisha Fayomi, Deepak Gupta, Vinay Kumar, Romany F. Mansour, Ensemble of deep learning based clinical decision support system for chronic kidney disease diagnosis in medical internet of things environment, Comput. Intell. Neurosci. 2021 (2021) 4931450, http://dx.doi.org/10.1155/2021/4931450.

[6] Andrea Facchinetti, Giovanni Sparacino, Stefania Guerra, Yoeri M. Luijf, J. Hans DeVries, Julia K. Mader, Martin Ellmerer, Carsten Benesch, Lutz Heinemann, Daniela Bruttomesso, et al., Real-time improvement of continuous glucose monitoring accuracy: the smart sensor concept, Diabetes Care 36 (4) (2013) 793–800, http://dx.doi.org/10.2337/dc12-0736.

[7] Ke Li, Cristiano Cardoso, Angel Moctezuma-Ramirez, Abdelmotagaly Elgalad, Emerson Perin, Heart rate variability measurement through a smart wearable device: Another breakthrough for personal health monitoring? Int. J. Env. Res. Public Heal. 20 (24) (2023) 7146, http://dx.doi.org/10.3390/ijerph20247146.

[8] Milena Georgieva, Charilaos Xenodochidis, Natalia Krasteva, Old age as a risk factor for liver diseases: Modern therapeutic approaches, Exp. Gerontol. 184 (2023) 112334, http://dx.doi.org/10.1016/j.exger.2023.112334.

[9] Vishal Chaudhary, Bakr Ahmed Taha, Lucky, Sarvesh Rustagi, Ajit Khosla, Pagona Papakonstantinou, Nikhil Bhalla, Nose-on-chip nanobiosensors for early detection of lung cancer breath biomarkers, ACS Sens. 9 (9) (2024) 4469–4494, http://dx.doi.org/10.1021/acssensors.4c01524.

[10] Chaman Verma, Zoltán Illés, Deepak Kumar, Using machine learning to predict satisfaction of students toward hybrid learning, in: Proc. 2023 Int. Conf. Innovation Intell. Informat., Comput., Technol., 3ICT, IEEE, 2023, pp. 88–93, http://dx.doi.org/10.1109/3ICT58811.2023.10380350.

[11] A.J.M. Rani, S. Nishanthini, D.C.J. Josephine, H. Venugopal, S.G. Nissi, V. Jacintha, Liver disease prediction using semi-supervised based machine learning algorithm, in: Proc. 2022 3rd Int. Conf. Smart Electron. Commun., ICOSEC, 2022, pp. 1389–1392, http://dx.doi.org/10.1109/ICOSEC54921.2022.9952144.

[12] K. Prakash, S. Saradha, A hybrid approach for prediction and stage-wise classification of liver failure, in: Proc. 2022 7th Int. Conf. Commun. Electron. Syst., ICCES, 2022, pp. 1679–1685, http://dx.doi.org/10.1109/ICCES54183.2022.9835913.

[13] Saqib A. Farooq, The multi-class detection of five stages of hepatitis c using the machine learning-based random forest algorithm, in: Proc. IEEE World Conf. Commun. Comput., 2023, pp. 1–6, http://dx.doi.org/10.1109/WCONF58270.2023.10235157.

[14] Francisco Valente, Simão Paredes, Jorge Henriques, Teresa Rocha, Paulo de Carvalho, João Morais, Interpretability, personalization and reliability of a machine learning based clinical decision support system, Data Min. Knowl. Discov. 36 (3) (2022) 1140–1173, http://dx.doi.org/10.1007/s10618-022-00821-8.

[15] Rudresh Dwivedi, Devam Dave, Het Naik, Smiti Singhal, Rana Omer, Pankesh Patel, Bin Qian, Zhenyu Wen, Tejal Shah, Graham Morgan, Rajiv Ranjan, Explainable AI (XAI): Core ideas, techniques, and solutions, ACM Comput. Surv. 55 (9) (2023) 1–33, http://dx.doi.org/10.1145/3561048.

[16] W. James Murdoch, Chandan Singh, Karl Kumbier, Reza Abbasi-Asl, Bin Yu, Interpretable machine learning: Definitions, methods, and applications, Proc. Natl. Acad. Sci. U. S. A. 116 (44) (2019) 22071–22080, http://dx.doi.org/10.1073/pnas.1900654116.

[17] Greeshma Arya, Ashish Bagwari, Hiteshi Saini, Prachi Thakur, Ciro Rodriguez, Pedro Lezama, Explainable AI for enhanced interpretation of liver cirrhosis biomarkers, IEEE Access (2023) http://dx.doi.org/10.1109/ACCESS.2023.3329759.

[18] Patrick S. Kamath, Clinical approach to the patient with abnormal liver test results, Mayo Clin. Proc. 71 (11) (1996) 1089–1095, http://dx.doi.org/10.4065/71.11.1089.

[19] Samuel Goldfischer, Herbert Popper, Irwin Sternlieb, The significance of variations in the distribution of copper in liver disease, Am. J. Pathol. 99 (3) (1980) 715–730, http://dx.doi.org/10.1016/S0002-9440(10)63107-5.

[20] Elizabeth E. Powell, Julie R. Jonsson, Andrew D. Clouston, Steatosis: Co-factor in other liver diseases, Hepatology 42 (1) (2005) 5–13, http://dx.doi.org/10.1002/hep.20750.

[21] Elmar Aigner, Michael Strasser, Heike Haufe, Thomas Sonnweber, Florian Hohla, Andreas Stadlmayr, Marc Solioz, Herbert Tilg, Wolfgang Patsch, Guenter Weiss, Felix Stickel, Christian Datz, A role for low hepatic copper concentrations in nonalcoholic fatty liver disease, Am. J. Gastroenterol. 105 (9) (2010) 1978–1985, http://dx.doi.org/10.1038/ajg.2010.170.

[22] Chenyan Yu, Yao Li, Minyue Yin, Jingwen Gao, Liting Xi, Jiaxi Lin, Lu Liu, Huixian Zhang, Airong Wu, Chunfang Xu, et al., Automated machine learning in predicting 30-day mortality in patients with non-cholestatic cirrhosis, J. Pers. Med. 12 (11) (2022) 1930, http://dx.doi.org/10.3390/jpm12111930.

[23] Giacomo Zaccherini, Emmanuel Weiss, Richard Moreau, Acute-on-chronic liver failure: Definitions, pathophysiology and principles of treatment, JHEP Rep. 3 (1) (2021) 100176, http://dx.doi.org/10.1016/j.jhepr.2020.100176.

[24] Junfeng Peng, Mi Zhou, Chuan Chen, Xiaohua Xie, Ching-Hsing Luo, Identification of exacerbation risk in patients with liver dysfunction using machine learning algorithms, PLoS One 15 (10) (2020) e0239266, http://dx.doi.org/10.1371/journal.pone.0239266.

[25] Aaron Fisher, Cynthia Rudin, Francesca Dominici, All models are wrong, but many are useful: Learning a variable's importance by studying an entire class of prediction models simultaneously, J. Mach. Learn. Res. 20 (177) (2019) 1–81, http://dx.doi.org/10.48550/arXiv.1801.01489.

[26] Scott M. Lundberg, Gabriel Erion, Hugh Chen, Alex DeGrave, Jordan M. Prutkin, Bala Nair, Ronit Katz, Jonathan Himmelfarb, Nisha Bansal, Su-In Lee, From local explanations to global understanding with explainable AI for trees, Nat. Mach. Intell. 2 (1) (2020) 56–67, http://dx.doi.org/10.1038/s42256-019-0138-9.

[27] fedesoriano, Cirrhosis prediction dataset, 2023, https://www.kaggle.com/datasets/fedesoriano/cirrhosis-prediction-dataset. (Accessed 2 February 2025).

[28] Walter Reade, Ashley Chow, Multi-class prediction of cirrhosis outcomes, 2023, Kaggle dataset URL https://www.kaggle.com/competitions/playground-series-s3e26/data. (Accessed 2 February 2025).

[29] Qusai Onali, Om Brahmbhatt, Trupal Chaudhary, Development of a machine learning model for envisaging cirrhosis mortality outcomes, Int. J. Res. Eng. Sci. Manag. 4 (8) (2021) 229–233.

[30] Mubarak Albarka Umar, Ali Nawaz, Tariq Qayyum, LRCMP: A sequential statistical framework for predicting cancer mortality rate, in: 2023 7th International Multi-Topic ICT Conference, IMTIC, IEEE, 2023, pp. 1–8, http://dx.doi.org/10.1109/IMTIC59016.2023.10182039.

[31] Pandiaraj Manickam, Siva Ananth Mariappan, Sindhu Monica Murugesan, Shekhar Hansda, Ajeet Kaushik, Ravikumar Shinde, S.P. Thipperudraswamy, Artificial intelligence (AI) and internet of medical things (IoMT) assisted biomedical systems for intelligent healthcare, Biosensors 12 (8) (2022) 562, http://dx.doi.org/10.3390/bios12080562.

[32] Farman Ali, Shaker El-Sappagh, S. M. Riazul Islam, Daehan Kwak, Amjad Ali, Muhammad Imran, Kyung-Sup Kwak, A smart healthcare monitoring system for heart disease prediction based on ensemble deep learning and feature fusion, Inf. Fusion 63 (2020) 208–222, http://dx.doi.org/10.1016/j.inffus.2020.06.008.

[33] Yoon Kim, Jinserk Seo, So-Yeon An, Dong Hyun Sinn, Ji Hye Hwang, et al., Efficacy and safety of an mHealth app and wearable device in physical performance for patients with hepatocellular carcinoma: Development and usability study, JMIR Mhealth UHealth 8 (3) (2020) e14435, http://dx.doi.org/10.2196/14435.

[34] Andreas Voss, Rico Schroeder, Steffen Schulz, Jens Haueisen, Stefanie Vogler, Paul Horn, Andreas Stallmach, Philipp Reuken, Detection of liver dysfunction using a wearable electronic nose system based on semiconductor metal oxide sensors, Biosensors 12 (2) (2022) 70, http://dx.doi.org/10.3390/bios12020070.

[35] Kaidong Wang, Samuel Margolis, Jae Min Cho, Shaolei Wang, Brian Arianpour, Alejandro Jabalera, Junyi Yin, Wen Hong, Yaran Zhang, Peng Zhao, Enbo Zhu, Srinivasa Reddy, Tzung K. Hsiai, Non-invasive detection of early-stage fatty liver disease via an on-skin impedance sensor and attention-based deep learning, Adv. Sci. 11 (31) (2024) e2400596, http://dx.doi.org/10.1002/advs.202400596.

[36] Debadatta Sengupta, Satarupa Mondal, Saurav Basu, Abhijit K. De, Sudip Nath, Ankit Pandey, Classification of acute liver failure using machine learning algorithms, in: Proc. IEEE Int. Conf. Electron. Comput. Commun. Technol., CONECCT, IEEE, 2022, pp. 1–6, http://dx.doi.org/10.1109/CONECCT55679.2022.9865744.

[37] Mohammad Ayoub Khan, An IoT framework for heart disease prediction based on MDCNN classifier, IEEE Access 8 (2020) 34717–34727, http://dx.doi.org/10.1109/ACCESS.2020.2974687.

[38] Abdul Hannan, Sehrish Munawar Cheema, Ivan Miguel Pires, Machine learning-based smart wearable system for cardiac arrest monitoring using hybrid computing, Biomed. Signal Process. Control. 87 (2024) 105519, http://dx.doi.org/10.1016/j.bspc.2023.105519.

[39] Deepak Kumar, Chaman Verma, Sanjay Dahiya, Pradeep K. Singh, Maria Simona Raboaca, Zoltán Illés, Brijesh Bakariya, Cardiac diagnostic feature and demographic identification (CDF-DI): An IoT enabled healthcare framework using machine learning, Sensors 21 (19) (2021) 6584, http://dx.doi.org/10.3390/s21196584.

[40] Arfat Ahmad Khan, Rakesh Kumar Mahendran, Usharani Thirunavukkarasu, Muhammad Faheem, D2PAM: Epileptic seizures prediction using adversarial deep dual-patch attention mechanism, CAAI Trans. Intell. Technol. 8 (3) (2023) 755–769, http://dx.doi.org/10.1049/cit2.12261.

[41] Arfat Ahmad Khan, Rakesh Kumar Mahendran, Kumar Perumal, Muhammad Faheem, Dual-3DM^3-AD: Mixed-transformer based semantic segmentation and triplet pre-processing for early multi-class alzheimer's diagnosis, IEEE Trans. Neural Syst. Rehabil. Eng. 32 (2024) 696–707, http://dx.doi.org/10.1109/TNSRE.2024.3357723.

[42] Ahmed Alhussen, Mohd Anul Haq, Arfat Ahmad Khan, Rakesh Kumar Mahendran, Seifedine Kadry, XAI-RACapsNet: Relevance aware capsule network-based breast cancer detection using mammography images via explainability O-net ROI segmentation, Expert Syst. Appl. 261 (2025) 125461, http://dx.doi.org/10.1016/j.eswa.2024.125461.

[43] Sudiksha Kottachery Kamath, Sanjeev Kushal Pendekanti, Divya Rao, LivMarX: An optimized low-cost predictive model using biomarkers for interpretable liver cirrhosis stage classification, IEEE Access 12 (2024) 92506–92522, http://dx.doi.org/10.1109/ACCESS.2024.3422451.

[44] Siva Sai, Aanchal Gaur, Vikas Hassija, Vinay Chamola, Artificial intelligence empowered digital twin and NFT-based patient monitoring and assisting framework for chronic disease patients, IEEE Internet Things Mag. 7 (2) (2024) 101–106, http://dx.doi.org/10.1109/iotm.001.2300138.

[45] Kumar Perumal, Rakesh Kumar Mahendran, Arfat Ahmad Khan, Seifedine Kadry, Tri-M2MT: Multi-modalities based effective acute bilirubin encephalopathy diagnosis through multi-transformer using neonatal magnetic resonance imaging, CAAI Trans. Intell. Technol. 10 (2) (2025) 434–449, http://dx.doi.org/10.1049/cit2.12409.

[46] Anima Kujur, Zahid Raza, Arfat Ahmad Khan Chen, Chitapong Wechtaisong, Data complexity based evaluation of the model dependence of brain MRI images for classification of brain tumor and alzheimer's disease, IEEE Access 10 (2022) 112117–112133, http://dx.doi.org/10.1109/ACCESS.2022.3216393.

[47] Vincent Croquet, Eric Vuillemin, Catherine Ternisien, Christophe Pilette, Frédéric Oberti, Yves Gallois, Marc Trossaert, Marie Christine Rousselet, Daniel Chappard, Paul Calès, Prothrombin index is an indirect marker of severe liver fibrosis, Eur. J. Gastroenterol. Hepatol. 14 (10) (2002) 1133–1141, http://dx.doi.org/10.1097/00042737-200210000-00015.

[48] Nadim Mahmud, Zachary Fricker, Rebecca A. Hubbard, George N. Ioannou, James D. Lewis, Talia H. Taddei, Kevin D. Rothstein, Michael Serper, David S. Goldberg, David E. Kaplan, Risk prediction models for post-operative mortality in patients with cirrhosis, Hepatology 73 (1) (2021) 204–218, http://dx.doi.org/10.1002/hep.31558.

[49] Honggang Zhang, Qinqin Sun, Weilin Mao, Jian Fan, Bo Ye, et al., Neutrophil-to-lymphocyte ratio predicts early mortality in patients with HBV-related decompensated cirrhosis, Gastroenterol. Res. Pr. 2016 (2016) 4394650, http://dx.doi.org/10.1155/2016/4394650.

[50] Shiming He, Song Lu, Changhui Yu, Maobin Kuang, Jiajun Qiu, Guotai Sheng, Yang Zou, The newly proposed plasma-glycosylated hemoglobin A1c/high-density lipoprotein cholesterol ratio serves as a simple and practical indicator for screening metabolic associated fatty liver disease: an observational study based on a physical examination population, BMC Gastroenterol. 24 (1) (2024) 274, http://dx.doi.org/10.1186/s12876-024-03362-0.

[51] Hyun-Cheol Park, YunSang Joo, O.-J. Lee, Kunkyu Lee, Tai-Kyong Song, Changhyun Choi, Moon Hyung Choi, Changhan Yoon, Automated classification of liver fibrosis stages using ultrasound imaging, BMC Med. Imaging 24 (1) (2024) 36, http://dx.doi.org/10.1186/s12880-024-00768-x.

[52] Mehdi Mohamadnejad, Seyed Mohammad Tavangar, Masoud Sotoudeh, Farid Kosari, Mohammad Khosravi, Behnam Geramizadeh, Gholam Montazeri, Ali Estakhri, Mohammad Mehdi Mirnasseri, Amirhossein Fazlollahi, et al., Histopathological study of chronic hepatitis b: A comparative study of ishak and METAVIR scoring systems, Int. J. Organ Transpl. Med. 1 (4) (2010) 171–176, http://dx.doi.org/10.24200/ijotm.2010.171.

[53] Tim Hulsen, Sharing is caring—Data sharing initiatives in healthcare, Int. J. Env. Res. Public Heal. 17 (9) (2020) 3046, http://dx.doi.org/10.3390/ijerph17093046.

[54] Kerim Koc, Role of Shapley additive explanations and resampling algorithms for contract failure prediction of public–private partnership projects, J. Manag. Eng. 39 (5) (2023) 04023031, http://dx.doi.org/10.1061/JMENEA.MEENG-5492.

[55] Giuseppe Casalicchio, Christoph Molnar, Bernd Bischl, Visualizing the feature importance for black box models, in: Lect. Notes Comput. Sci., vol. 11051, Springer, 2019, pp. 655–670, http://dx.doi.org/10.1007/978-3-030-10925-7_40.

[56] Amazon Web Services, AWS Pricing Calculator, 2025, URL https://aws.amazon.com/aws-cost-management/aws-pricing-calculator/. (Accessed 18 May 2025).

[57] Badrinath Jagannath, Kai-Chun Lin, Madhavi Pali, Devangsingh Sankhala, Sriram Muthukumar, Shalini Prasad, Temporal profiling of cytokines in passively expressed sweat for detection of infection using wearable device, Bioeng. Transl. Med. 6 (3) (2021) e10220, http://dx.doi.org/10.1002/btm2.10220.

[58] Hanah Kim, Mina Hur, Giuseppe d'Onofrio, Gina Zini, Real-world application of digital morphology analyzers: Practical issues and challenges in clinical laboratories, Diagnostics 15 (6) (2025) 677, http://dx.doi.org/10.3390/diagnostics15060677.

[59] Nicholas X. Williams, Brittani Carroll, Steven G. Noyce, Hansel A. Hobbie, Daniel Y. Joh, Joseph G. Rogers, Aaron D. Franklin, Fully printed prothrombin time sensor for point-of-care testing, Biosens. Bioelectron. 172 (2021) 112770, http://dx.doi.org/10.1016/j.bios.2020.112770.

[60] Anubhuti Saha, Ashutosh Bajpai, Vinay Krishna, Shantanu Bhattacharya, Evolving paradigm of prothrombin time diagnostics with its growing clinical relevance towards cardio-compromised and COVID-19 affected population, Sensors 21 (8) (2021) 2636, http://dx.doi.org/10.3390/s21082636.

[61] Xiao-Lu Xu, Shun-Xin Li, Ying Yang, Xiang-Chao Sun, Hong Xia, High-performance strain sensor for detection of human motion and subtle strain by facile fabrication, Measurement 189 (2022) 110658, http://dx.doi.org/10.1016/j.measurement.2021.110658.

[62] Andres Ruf, Melisa Dirchwolf, Richard B. Freeman, From child-pugh to MELD score and beyond: Taking a walk down memory lane, Ann. Hepatol. 27 (1) (2022) 100535, http://dx.doi.org/10.1016/j.aohep.2021.100535.
[63] Abdelmlak Said, Aymen Yahyaoui, Takoua Abdellatif, HIPAA and GDPR compliance in IoT healthcare systems, in: Advances in Model and Data Engineering in the Digitalization Era, in: Commun. Comput. Inf. Sci., vol. 2071, 2024, pp. 198–209, http://dx.doi.org/10.1007/978-3-031-55729-3_16.
[64] Koushal Sattaru, Mansi Thipani Madhu, Janmejay Kumar Singh, Venkataramana Kandi, Aastha Gupta, C.A. Jayashankar, et al., A comprehensive review of the effects of diabetes mellitus on the gastrointestinal system, Cureus 17 (1) (2025) e77845, http://dx.doi.org/10.7759/cureus.77845.
[65] Tianci Wen, Yongchun Fang, Biao Lu, Xuebo Zhang, Chaoquan Tang, LIVER: A tightly coupled LiDAR–Inertial–Visual state estimator with high robustness for underground environments, IEEE Robot. Autom. Lett. 9 (3) (2024) 2399–2406, http://dx.doi.org/10.1109/LRA.2024.3355778.
[66] Barbara Daniel, Godwin James, Cloud data privacy: Trends, challenges, and future outlook, 2023.
[67] Shekha Chenthara, Khandakar Ahmed, Frank Whittaker, Privacy-preserving data sharing using multi-layer access control model in electronic health environment, EAI End. Trans. Scalable Inf. Syst. 6 (22) (2019) http://dx.doi.org/10.4108/eai.13-7-2018.159356.
[68] Zhaomin Chen, Chai Kiat Yeo, Bu-Sung Lee, Chiew Tong Lau, Autoencoder-based network anomaly detection, in: 2018 Wireless Telecommun. Symp., WTS, 2018, pp. 1–5, http://dx.doi.org/10.1109/WTS.2018.8363930.
[69] Wenhao Jiang, Hongchang Gao, Fu-Lai Chung, Heng Huang, The l2, 1-norm stacked robust autoencoders for domain adaptation, in: Proc. AAAI Conf. Artif. Intell., vol. 30, no. 1, AAAI Press, 2016, pp. 1723–1729, http://dx.doi.org/10.1609/aaai.v30i1.10274.
[70] Vahid Sinap, The impact of balancing techniques and feature selection on machine learning models for diabetes detection, Fırat Univ. Eng. Sci. J. 37 (1) (2025) 303–320, http://dx.doi.org/10.35234/fumbd.1556260.
[71] Rayene Bounab, Bouchra Guelib, Karim Zarour, A novel machine learning approach for handling imbalanced data: Leveraging SMOTE-ENN and XGBoost, in: Proc. 2024 6th Int. Conf. Pattern Anal. Intell. Syst., PAIS, 2024, pp. 1–7, http://dx.doi.org/10.1109/PAIS62114.2024.10541220.
[72] Ankan Kar, Nirjhar Nath, Utpalraj Kemprai, Aman, Performance analysis of support vector machine (SVM) on challenging datasets for forest fire detection, 2024, http://dx.doi.org/10.4236/ijcns.2024.172002, ArXiv Preprint arXiv:2401.12924. Also published in *Int. J. Commun. Netw. Syst. Sci.* 17, 11–29 (2024).
[73] Hasan Ahmed Salman, Ali Kalakech, Amani Steiti, Random forest algorithm overview, Babylon. J. Mach. Learn. 2024 (2024) 69–79, http://dx.doi.org/10.58496/BJML/2024/007.
[74] Soukaina Hakkal, Ayoub Ait Lahcen, XGBoost to enhance learner performance prediction, Comput. Educ.: Artif. Intell. (2024) 100254, http://dx.doi.org/10.1016/j.caeai.2024.100254.
[75] Tianqi Chen, Carlos Guestrin, XGBoost: A scalable tree boosting system, in: Proc. 22nd ACM SIGKDD Int. Conf. Knowl. Discov. Data Min., 2016, pp. 785–794, http://dx.doi.org/10.1145/2939672.2939785.
[76] Mucan Liu, Chonghui Guo, Liangchen Xu, An interpretable automated feature engineering framework for improving logistic regression, Appl. Soft Comput. 153 (2024) 111269, http://dx.doi.org/10.1016/j.asoc.2024.111269.
[77] K. Prakash, S. Saradha, A hybrid approach for prediction and stage wise classification of liver failure, in: 2022 7th Int. Conf. Commun. Electron. Syst., ICCES, IEEE, 2022, pp. 1679–1685, http://dx.doi.org/10.1109/ICCES54183.2022.9835913.
[78] Ankur Arya, Andrew Niederhausern, Nadia Bahadur, Neil J. Shah, Chelsea Nichols, Avijit Chatterjee, John Philip, Artificial intelligence–assisted cancer status detection in radiology reports, Cancer Res. Commun. 4 (4) (2024) 1041–1049, http://dx.doi.org/10.1158/2767-9764.CRC-24-0064.
[79] Julia Maroto-García, Ana Moreno Álvarez, María P. Sanz de Pedro, Antonio Buño-Soto, Álvaro González, Serum biomarkers for liver fibrosis assessment, Adv. Lab. Med. 5 (2) (2024) 115–130, http://dx.doi.org/10.1515/almed-2023-0081.
[80] Nikolaos Andreatos, Neda Amini, Faiz Gani, Georgios A. Margonis, Kazunari Sasaki, Vanessa M. Thompson, David J. Bentrem, Bruce L. Hall, Henry A. Pitt, Ana Wilson, et al., Albumin-bilirubin score: predicting short-term outcomes including bile leak and post-hepatectomy liver failure following hepatic resection, J. Gastrointest. Surg. 21 (2) (2017) 238–248, http://dx.doi.org/10.1007/s11605-016-3246-4.
[81] Ji Soo Choi, Kyung Soo Chung, Eun Hye Lee, Su Hwan Lee, Sang Hoon Lee, Song Yee Kim, Ji Ye Jung, Young Ae Kang, Moo Suk Park, Young Sam Kim, et al., The role of bilirubin to albumin ratio as a predictor for mortality in critically ill patients without existing liver or biliary tract disease, Acute Crit. Care 35 (1) (2020) 24, http://dx.doi.org/10.4266/acc.2019.00738.
[82] Leon Fisher, Wichat Srikusalanukul, Alexander Fisher, Paul Smith, Liver function parameters in hip fracture patients: relations to age, adipokines, comorbidities and outcomes, Int. J. Med. Sci. 12 (2) (2015) 100, http://dx.doi.org/10.7150/ijms.10696.
[83] Ahmad Anouti, Thomas A. Kerr, Mack C. Mitchell, Thomas G. Cotter, Advances in the management of alcohol-associated liver disease, Gastroenterol. Rep. 12 (2024) goae097, doi:10.10.1093/gastro/goae097.
[84] Dorina Osmanaj, Floreta Kurti, Klerida Shehu, Yllka Themeli, Gentian Stroni, Erand Llanaj, Adriana Babameto, Clinical characteristics of alcohol-related liver disease in Albanian patients: A cross-sectional study, Gastroenterol. Insights 16 (2) (2025) 16, http://dx.doi.org/10.3390/gastroent16020016.
[85] Mauro Bernardi, Carmen S. Ricci, Giacomo Zaccherini, Role of human albumin in the management of complications of liver cirrhosis, J. Clin. Exp. Hepatol. 4 (4) (2014) 302–311, http://dx.doi.org/10.1016/j.jceh.2014.08.007.
[86] Centers for Disease Control and Prevention (CDC) and National Center for Health Statistics (NCHS), National health and nutrition examination survey data, 2020, https://wwwn.cdc.gov/nchs/nhanes/continuousnhanes/default.aspx?Cycle=2017-2020. Hyattsville, MD: U.S. Department of Health and Human Services, Centers for Disease Control and Prevention.
[87] Qingling Chen, Pingping Hu, Xiaoxue Hou, Ye Sun, Mengfan Jiao, Linya Peng, Zixing Dai, Xizhi Yin, Rui Liu, Yuwen Li, et al., Association between triglyceride-glucose related indices and mortality among individuals with non-alcoholic fatty liver disease or metabolic dysfunction-associated steatotic liver disease, Cardiovasc. Diabetol. 23 (1) (2024) 232, http://dx.doi.org/10.1186/s12933-024-02343-7.
[88] Nikolaj Torp, Mads Israelsen, Minneke Coenraad, Maria Papp, Debbie Shawcross, Marko Korenjak, Paolo Angeli, Wim Laleman, Adria Juanola, Pere Gines, et al., Personalised human albumin in patients with cirrhosis and ascites: design and rationale for the ALB-TRIAL-a randomised clinical biomarker validation trial, BMJ Open 14 (2) (2024) e079309, http://dx.doi.org/10.1136/bmjopen-2023-079309.

Deepak Kumar is a dedicated academician and researcher with a strong focus on ML. He has made significant contributions to both the academic and research communities through various initiatives. His research spans a wide range of ML applications, with over 30 published research papers in esteemed international and national journals and conferences. He has since accumulated more than 17 years of teaching experience, making substantial contributions to academia. In addition to his teaching and research, he has demonstrated strong leadership through organizing key academic events and playing active roles in international conferences, serving as a session chair and keynote speaker.

Dr. Brijesh Bakariya is an Assistant Professor and Coordinator in the Department of Computer Science and Engineering, I.K. Gujral Punjab Technical University (IKG-PTU) Campus Hoshiarpur, Punjab. He completed his Ph. D. from the National Institute of Technology (NIT- Bhopal), Madhya Pradesh (2016). He received his MCA degree from Devi Ahilya Vishwavidyalaya (DAVV), Indore, Madhya Pradesh (2009). He has been teaching since 2009 and guiding M.Tech/Ph.D. students. In the meantime, he has authored 5 books and published more than 40 research papers in journals of international repute in Data mining, ML, Image processing, Human activity recognition, and so on. He published 06 patents, and out of these, 02 patents were granted. Currently, he supervises four Ph.D. scholars. He has attended various short-term training programs, refresher courses, workshops, seminars, and conferences in India.

Dr. Chaman Verma is an Assistant Professor at the Department of Media and Educational Informatics, Faculty of Informatics, Eötvös Loránd University. He is also the Project leader & Chief researcher of his project sponsored by National Research, Development and Innovation (NRDI) Hungary. He also won a young educator scholarship for novel research sponsored by the EKÖP, NRDI Fund, and the Hungarian Government. He pursued a postdoctorate at the faculty of informatics, Eötvös Loránd University, Budapest, Hungary, sponsored by UNKP, MIT (Ministry of Innovation and Technology), the National Research, Development and Innovation (NRDI) Fund, Hungarian Government. He received a Ph.D. in informatics from the Doctoral School of Informatics, Eötvös Loránd University, Budapest, Hungary, with the Stipendium Hunagricum Scholarship funded by the Tempus Public Foundation, Government of Hungary. During

his Ph.D., he won the EFOP Scholarship, CoFounded by the European Union Social Fund and the Government of Hungary, as a Professional Research Assistant in a real-time system from 2018 to 2021. He also received the Stipendium Hungaricum Dissertation Scholarship of Tempus Public Foundation, Government of Hungary, from 2021 to 2022. He has been awarded several Erasmus Scholarships for conducting international research and academic collaboration with European and non-European universities. He received the best Scientific Publication award from the faculty of informatics, Eötvös Loránd University, Budapest, Hungary, In the years 2021-2024. He has also been awarded the ÚNKP scholarship for research by the Ministry of Innovation and Technology and the National Research, Development and Innovation (NRDIO) Fund, Government of Hungary, 2021-2023. He has around ten years of experience in teaching and industry. He has over 150 scientific publications in the IEEE, Elsevier, Springer, IOP Science, Walter de Gruyter and MDPI. His research interests include data analytics, feature engineering, real-time systems, and educational informatics. He is a Life Member of ISTE, New Delhi, India. He is a member of the editorial board and a reviewer of various international journals and scientific conferences. He was the leading Guest Editor of the Special Issue Advancement in ML and Applications in Mathematics, IF2.25, MDPI, Basel, Switzerland, in 2022. He was also a guest editor in two Springer journals. He is a co-editor in the series of conference proceedings of ICRIC-2021-24 published by Springer, Singapore. He reviews many scientific journals, including IEEE, Springer, Elsevier, Wiley, and MDPI. He has Scopus citations of 1300 with an H-index of 21. He has Web of Science citations of 100 with an H-index of 10.

Zoltán Illés received the Ph.D. and Habilitation degrees in mathematics and physics from Eötvös Loránd University. Later, he took up the computer science supplementary course, which was started at that time. His Ph.D. dissertation was titled ‘‘Implementation of Real-Time Measurements for High-Energy Ion Radiations,’’ in 2001. After graduating in 1985, he joined the Department of Computer Science, Eötvös Loránd University. In 2004, at the request of Jedlik Publisher, he also wrote a textbook on the C programming language. This book has a second, expanded edition in 2008. He received a scholarship from the Slovak Academy of Sciences in 2007, and he spent six months conducting research and instructing at Constantine the Philosopher University in Nitra. The NJSZT awarded the Rezső Tarján Prize, in 2016, for the success of the joint work that has been going on ever since. He and his colleagues also researched the issue of mobile devices and applications in the framework of a tender won, in 2014. Based on their research findings, he launched a pilot project to support real-time, innovative performance management. The first results of this research are an integral part of the habilitation dissertation. He got a Hungarian Republic Scholarship based on his outstanding academic achievements during university studies. Since 2020, he has been an invited speaker at several international conferences and an Amity University Advisory Board Member.